esa

SP-1196 (8)

REPORTS FOR ASSESSMENT

THE NINE CANDIDATE EARTH EXPLORER MISSIONS

Precipitation Mission

SAMPLE

European Space Agency
Agence spatiale européenne

PLEASE DO NOT REMOVE

esa SP-1196 (8)
April 1996

REPORTS FOR ASSESSMENT

THE NINE CANDIDATE EARTH EXPLORER MISSIONS

Precipitation Mission

ESA SP-1196 (8) – The Nine Candidate Earth Explorer Missions –
PRECIPITATION MISSION

Report prepared by: Earth Sciences Division
Coordinator: Chris J. Readings

Earth Observation Preparatory Programme
Coordinator: Mike L. Reynolds

Cover: Richard Francis & Carel Haakman

Published by: ESA Publications Division
c/o ESTEC, Noordwijk, The Netherlands
Publication Manager: Tan-Duc Guyenne

ISBN 92-9092-383-0

Contents

1. Introduction 5

2. Background and Scientific Justification 7
2.1. Introduction 7
2.2. Scientific Requirements for Precipitation Data 7
2.3 Planned TRMM Mission 21
2.4. Proposed Precipitation Mission 26

3. Research Objectives 29
3.1. Requirements for Precipitation Data 29
3.2. Problems with Existing and Planned Data Sources 29
3.3. Requirements for the Proposed Precipitation Mission 30

4. Observational Requirements 33
4.1. Sampling 33
4.2. Radar Technique 35
4.3. Precipitation Microwave Radiometer 44
4.4. Synergy Between Instruments 45
4.5. Extension of the Upper Limit of the Dynamic Range 48
4.6. Exploitation of the Mission in the Absence of Rain 50
4.7 Summary of Observational Requirements 51

5. Mission Elements 53
5.1. The Precipitation Mission Elements 53
5.2. Satellite and Orbit 54
5.3. Ground Segment 54
5.4. Supporting Mission Elements 54

6. System Concept 55
6.1. General 55
6.2. Payload 55
6.3. Mission and Operations Profile 64
6.4. The Spacecraft 65
6.5. Ground Segment and Data Processing 69
6.6. Launcher 71
6.7. Implementation Option 72

7. Programmatics 75
7.1. General 75
7.2. Critical Areas and Open Issues 75
7.3. Related Missions and Timeliness 75
7.4. International Cooperation 76
7.5. Enhancement of European Capabilities and Applications Potential 76

References 77

List of Acronyms 81

1. Introduction

For the post 2000 time frame two general classes of Earth Observation missions have been identified to address user requirements, namely:

Earth Explorer Missions – these are research/demonstration missions with the emphasis on advancing understanding of the different Earth system processes. The demonstration of specific new observing techniques would also fall under this category.

Earth Watch Missions – these are pre-operational missions addressing the requirements of specific Earth observation application areas. The responsibility for this type of mission would eventually be transferred to operational (European) entities and the private sector.

Nine Earth Explorer missions have been identified as potential candidates for Phase A study. For each of these candidate missions Reports for Assessment have been produced.

This particular Report for Assessment is concerned with the Earth Explorer Precipitation Mission. It has been prepared by one of the nine Mission Working Groups that have been established to produce these Reports. The four (external non-ESA) members of this particular Mission Working Group are Anthony Illingworth (University of Reading, Reading, United Kingdom), Klaus Arpe (Max-Planck Instut für Meteorologie, Hamburg, Germany), Alberto Mugnai (CNR, Instituto di Fisica dell'Atmosfera, Frascati, Italy), and Jacques Testud (CRPE, Centre Universitaire de Velizy, Velizy, France). They were supported by members of the Agency who advised on technical aspects and took the lead in drafting technical/programmatic sections. This Report, together with the other eight candidate Earth Explorer missions, is being circulated amongst the Earth Observation research community in anticipation of a Workshop which will be held in Spain in May 1996.

The major thrust for this mission comes from the lack of knowledge of present precipitation over the Earth, the difficulty in representing precipitation processes in models used for climate and weather prediction, and the consequent uncertainty in predicting rainfall patterns in a changing future climate. The top priority is to provide accurate rainfall measurements to validate the precipitation schemes in climate and weather prediction models. Most of the worldwide precipitation falls at latitudes between +/- 60°, over two thirds in the tropics (+/– 30°). This is a major source of energy driving the global circulation. The proposed Earth Explorer Precipitation Mission would focus on the observation of precipitation in these latitudes.

All the Reports for Assessment follow a common general structure comprising seven chapters. They each start by addressing the scientific justification for particular mission and move on to detail the specific objectives. This is followed by a detailing of the specification of observation requirements and a listing of the various mission elements required to satisfy the observational requirements. Then consideration is given to the implications of meeting the observational requirements in terms of both the space and ground segment as well as requisite advances in scientific algorithms and processing/assimilation techniques. Finally programmatic aspects are considered.

2. Background and Scientific Justification

2.1. Introduction

Precipitation is a crucial element affecting human life on Earth, but because of its great variability in space and time it is one of the most difficult to observe. The correct representation of precipitation processes is vital in numerical models which are used both for simulating climate and also in numerical weather prediction. Global measurements of surface precipitation and its vertical structure are required to validate and improve these models.

The knowledge of global precipitation is unsatisfactory; there are sparse data over land and virtually no data over the sea. Satellites are the only means of providing complete precipitation data sets over the oceans, yet current rainfall retrievals from passive satellite instruments are not sufficiently reliable. Accurate co-located observations are needed for tuning and validation of retrieval methods.

The Tropical Rainfall Measuring Mission (TRMM) is planned for launch in 1997, and should provide the first data from a spaceborne active range-gated rain radar. A TRMM follow-on called ATMOS A1 is under consideration by Japan.

2.2. Scientific Requirements for Precipitation Data

2.2.1. Present Use of Precipitation Data

A main emphasis in climate research has been to simulate the atmosphere and ocean with numerical models. Such models can investigate the response of the atmosphere and the ocean under different external forcings such as the increase of carbon dioxide. For gaining confidence in these models one has to validate them under present conditions; a key variable is precipitation and so one needs climatological data in the form of long term means and also measures of variability. The correct representation of precipitation processes within General Circulation Models (GCMs) used for Numerical Weather Prediction (NWP) is also a crucial problem. Another way of validating such models is to check that they correctly represent the spatial and temporal distribution of precipitation at a particular time.

Present Sources of Global Precipitation Data

At the Global Precipitation Climate Centre (GPCC) in Offenbach attempts are under way to collect all regional archives to a global archive and to merge them together with operational observations to a global gridded data set. It is the goal of the Global Precipitation Climatology Project (GPCP) to produce global distributions of monthly means on a $2.5 \times 2.5^\circ$ grid. For that GPCC has already produced a 9 year series based on ground observations. This land-based data set will have large areas without any ground-based observations and these have to be filled with other data i.e. data from satellite observations. Even then there are gaps in the data coverage, especially in polar regions, and therefore model output from operational weather forecasting centres or re-analysis projects have to be used to gain a complete global coverage. Improved techniques for estimating rainfall are being validated by intercomparison campaigns (AIP, algorithm intercomparison project and PIP, precipitation intercomparison project).

Widely used data sets are the climatological means of precipitation and 2-metre temperatures by Legates and Willmott (1990). These climatological means show obvious deficiencies and there are concerns over their reliability. The GPCP data set will soon span over a period of 10 years and can then be averaged to obtain a new and probably more realistic climatology, however, because of a large inter-decadal variability of precipitation it will still not provide a real climatological mean and the absolute accuracy is still insufficient, especially for oceanic areas.

The estimates of precipitation provided by operational weather forecasts can hardly be called observations, but, at the moment, they are the only data source which provides a global coverage on a daily basis (even 6 hourly). Their quality has improved considerably in recent years. Monthly means of precipitation from analysis/forecasting centres in the short range may be of similar accuracy as present analyses based solely on observed precipitation.

Precipitation in polar regions is perhaps least well known. As the amounts are small, its contribution to the total energy budget of the atmosphere is less important. When simulating the future climate, a feed back through the albedo from the snow on the ground and on sea-ice may play an important role and it may be more important than recognized in the past to be able to validate the precipitation in polar regions. Also the question of glacier advance or melting is recognized as becoming important. Snow on sea ice is important for the energy exchange between the ocean and the atmosphere and for melting sea ice.

In Figure 2.1 the two best estimates of precipitation over the northern hemisphere are shown. The patterns are quite similar over the American continent but the actual values differ often by a factor of 2. Over the oceans differences can be very large, e.g. over the northern Pacific storm track where ERA generates values of up to 5 mm/day while the analysis (based in this area on SSM/I observations) reaches only 2 mm/day. Around Hawaii the problem of extrapolating ground-based observations to ocean areas is obvious. Over the Atlantic even the patterns lack similarities.

Representation of Precipitation Within Models

The advanced global circulation models (GCMs) used for climate research and NWP carry cloud water as a prognostic variable, but not precipitating water. Ground precipitation is

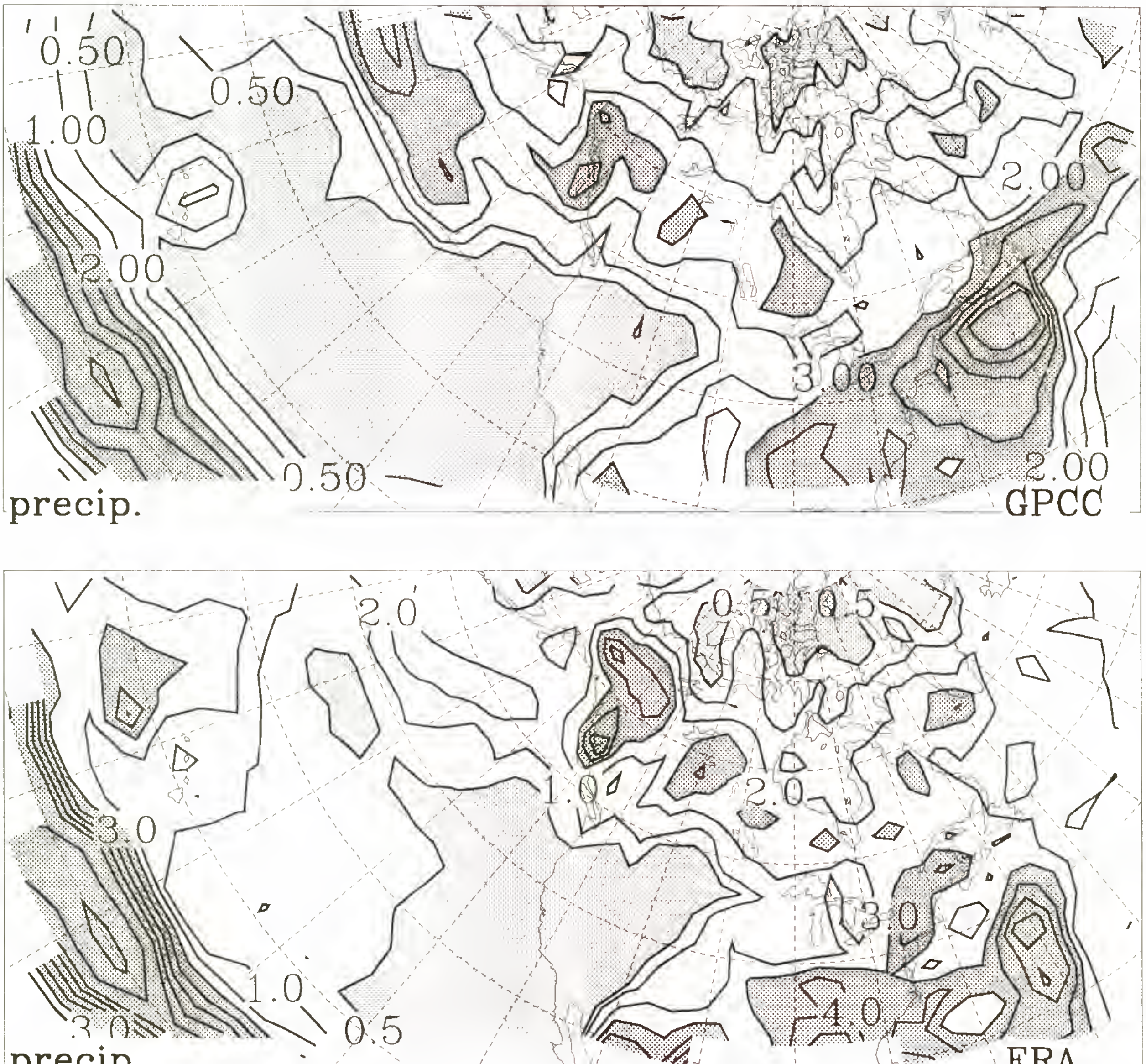

Figure 2.1: *Precipitation in July 1988 estimated by GPCC and generated during the first guess forecasts for the ECMWF re-analysis (ERA). Contours at 0.5, 1, 2, 3, 4, 5, 6, 7, 10, 15, 20, 25, 30 mm/day. Shading for precipitation rates greater than 3 and lower than 0.5 mm/hour.*

forecast as a combination of grid scale and subgrid scale contributions (subgrid scale is a by-product of the convective scheme). It is possible that within ten years, such models would carry precipitating water as well (as is presently done in detailed cloud models). The detailed processes involved in the production of precipitation cannot be represented within the models, but instead they are parameterised into much simpler expression. Initially rain data will be used to check that climate models give the present day precipitation. Rain data will also be used for the validation of NWP forecasts, but on a longer term, it is anticipated that rain will be assimilated in GCMs using, for example, the four dimensional variational method.

Validation data will be more valuable if it distinguishes between convective and stratiform precipitation as they are represented differently in the models. Information about vertical profiles of precipitation and consequent vertical transport of latent heat is also needed for validation. In the mid-latitude oceanic storm tracks large amounts of latent heat are released which are extremely important for forecasting the weather in Europe. The availability of precise observations including vertical profiles in an operational environment would provide numerous occasions to validate and improve the parameterisation of precipitation processes within the model. Large differences between model predictions and observations will indicate where improvements are needed.

Finally, it is noted that biochemical and hydrological models need precipitation observations for tuning with requirements for statistical information of the variability of precipitation with a very fine scale in time and space.

Time Scales of Variability

For investigating the variability of climate one needs very long series of observations (many decades) which are not affected by changes in the observational method nor in the treatment of the data. Presently available data sets are restricted to land areas but even there one does not get a complete coverage. The number of observational stations which fulfil the requirement of unchanged observational methods for very long periods is clearly limited.

Shorter time series of monthly or seasonal means (10-20 years) are used for investigating the interannual variability, especially the impact of Sea Surface Temperature (SST) on the atmospheric circulation and connected with that on the precipitation is studied, also in connection with model simulations. The variability of precipitation over India is a good example. Statistical methods are used to find correlations between precipitation and other quantities, e.g. the SST over the Indian or Pacific Oceans or the snow depth over Siberia.

The mean diurnal cycle and its variation through the year is needed for model validation, but is presently only known with a high margin of uncertainty.

Hydrological models need statistics about variabilities of precipitation in time and space on a very fine scale within grid boxes which are hardly known except for very few areas.

In the light of investigations of the future climate it is important to check that the model simulates present conditions with the correct frequency distributions of precipitation intensities so that extreme events, such as periods of drought and heavy rain leading to flooding are correctly represented and understood. For example, the Rhine river has had recently two so called "century events" of floods.

The World Climate Research Programme (WCRP) has addressed the importance of arctic precipitation by initiating the Arctic climate system (ACSYS) project.

2.2.2. Shortcomings of Present Rainfall Data (Climate and Instantaneous)

The only data on vertical profiles of precipitation is from a few ground-based and air-borne radars.

Deficiencies of Ground-Based Observations

Ground-based observations are sparse, being restricted to small areas of the globe. There are no data over a large fraction of the land, and none at all over the open ocean. Rainfalls from gauges are essentially point measurements, and because of the great spatial variability of rainfall are not usually representative of rainfall over an area. The representativity problem compounds the difficulty of interpolating such point measurements on to a regular grid. In addition, the gauges themselves may have errors due to wind and exposure problems, difficulties which are exacerbated during snowfall and over mountainous areas.

Precipitation Inferred from Visible/Infrared Satellite Observations

Visible/Infrared (VIS/IR) radiation upwelling from clouds, and eventually measured by space-borne radiometers, is reflected/emitted by the top layers of the cloud and it is (at most) weakly correlated to the microphysical structure of the underlying cloud and precipitation layers. Thus, VIS/IR precipitation retrieval algorithms can not be based on information directly associated with precipitation, but are based on the fact that high and thick – i.e., highly reflective and radiometrically cold (for VIS/IR radiation, respectively) – clouds are associated with precipitation, particularly in convective systems.

Some techniques try to overcome this inherent deficiency of information by relating cloud height and thickness to precipitation at the surface by means of additional information, such as cloud top textural structure and/or temporal variations in cloud top height or cloud size. Other IR techniques, such as the Geostationary Operational Environment Satellite (GOES) Precipitation Index (GPI) (e.g. Arkin et al., 1994) make use of brightness temperature (T_B) thresholds to separate rainy from non rainy pixels (the original GPI uses a single, fixed threshold of 235 K to associate a mean rain rate of 3 mm/hour to all pixels with $T_B < 235$ K). This method can only be used in the tropics.

In all cases VIS/IR techniques must be calibrated using direct measurements of precipitation (e.g. radar measurements). In this process, geographically and/or seasonally dependent coefficients and/or thresholds should be used in order to adapt the techniques to different climatological rain rate regimes; otherwise, significant errors may be generated when the techniques are used for regions and/or seasons different from the ones considered for their calibration.

Precipitation Estimated from Passive Microwave Satellite Observations

Passive microwave (MW) measurements from space have, in principle, great potential for estimating precipitation because the upwelling radiation over the precipitating cloud is directly responsive, in a frequency dependent fashion, to precipitation microphysics. However, due to the complexity of the problem and to difficulties related to the characteristics of the radiometers that have been used so far, quantification of precipitation from satellite passive microwave radiance data still remains, to a large extent, unresolved. Several algorithms for the retrieval of precipitation have been proposed in the last decade or so, a consensus algorithm has yet to be developed by the scientific community (for a brief description of several passive microwave algorithms, mostly based on the DMSP-SSM/I (Defence Meteorological Satellite Program – Special Sensor Microwave Imager) image data, and one based on the NOAA-MSU (Microwave Sounding Unit) vertical profile data, see Wilheit et al., 1994). This observes at 19.35, 22.235, 37.0, and 85.5 GHz (see e.g. Hollinger et al, 1990). It is presently flown on a sun-synchronous, near-polar orbit spacecraft.

Data furnished by SSM/I have been used to provide estimates of precipitation, but suffer from problems that are not only due to deficiencies of the retrieval techniques themselves, but are also due to the characteristics of the instrument such as the SSM/I's space and temporal sampling, which is not adequate for correct observation of precipitation, as well as its frequency selection and scan geometry.

There are two problems for the spatial sampling:

1) The SSM/I's daily global coverage presents large diamond-shaped areas at the equator that are not observed (but will be covered after 72 hours); and
2) the footprint size, which is too large, mainly at the lower frequencies (it ranges from 13 km × 15 km at 85.5 GHz up to 43 km × 69 km at 19.35 GHz), for adequately resolving the spatial variability of precipitation.

In particular, the footprint size problem complicates precipitation retrieval for three reasons:

1) errors arising if the beam is not uniformly filled with precipitation
2) possible background variations within a pixel (especially over land, where surface emissivity characteristics may be highly variable)
3) difficulties arise with multifrequency methods because the footprint size is highly dependent on frequency with a maximum resolution at 85.5 GHz.

To achieve improved resolution at the low frequencies, antenna pattern deconvolution need to be applied, however, SSM/I has sampling characteristics that allow deconvolution only for the 19 GHz channels.

The temporal sampling of a polar orbiting spacecraft affects the average estimates of precipitation because any location over the Earth is observed (usually, at most twice a day) at about the same local times and therefore the daily cycle can not be resolved. While geostationary microwave radiometers would be the optimal solution for this problem, high frequencies (> 90 GHz) are needed to provide reasonable spatial resolution, but these frequencies are mainly influenced by the top portions of the observed clouds rather than the precipitation.

The SSM/I does not have a 10.7 GHz channel. This frequency is important for retrieving medium-to-high precipitation over the ocean – as measurements taken by the AMPR (Advanced Microwave Precipitation Radiometer) (Spencer et al.,1994) clearly show - but from a satellite the large footprint size make its use problematic. The TRMM Microwave Imager (TMI), will include the 10.7 GHz frequency, in addition to the four SSM/I frequencies but with twice the ground resolution.

The SSM/I scan geometry (a 45° conical scan with a constant incidence angle at the Earth surface) presents one advantage for precipitation retrieval (due to the constant incidence angle of 53.1°, retrieval procedures do not have to be changed when moving from one pixel to the next) and two disadvantages that are related to the fact that observations are (largely) off-nadir. First, since the various frequencies penetrate differently through the precipitating cloud (the lower the frequency, the larger the penetration towards cloud bottom), their use in a multifrequency retrieval scheme is partly incorrect because they "see" different portions of different cloud columns, rather than of the same column – thus, microphysical consistency is partially lost. Second, off-nadir observations may make beam-filling problems more severe, especially when considering complex three-dimensional cloud systems over the ocean (due to its low emissivity/large reflectivity characteristics).

The Global Precipitation Climatology Project and Algorithm Intercomparisons

The goal of the Global Precipitation Climatology Project (GPCP) is to produce a 10 year set of monthly analyses of areal-averaged precipitation on a 2.5° global grid. Because of the empirical nature of the satellite algorithms several algorithm intercomparison projects (AIPs) and precipitation intercomparison projects (PIPs) have been carried out.

From the three AIPs carried out in Japan, North-West Europe and the Western Pacific the main conclusions from comparison of satellite estimates with ground truth are (Ebert et al., 1996):

1) the skill of the various algorithms for estimating precipitation from satellite depends on

the regime being analyzed (i.e., for instance, some algorithms performed very well over the tropical western Pacific and over Japan, but relatively poorly for springtime precipitation over Western Europe)
2) monthly rainfall was estimated slightly better by geostationary (IR, VIS/IR, and mixed IR-SSM/I) algorithms due to better sampling; however,
3) instantaneous rain rates were estimated much better by SSM/I algorithms (especially outside the tropics) because of physical links between microwave measurements and precipitation microphysics; and, finally,
4) while in the European case NWP forecasts outperformed all satellite algorithms, the opposite was true for the tropical western Pacific.

The findings of the AIPs indicate that current precipitation estimates derived from IR satellites are not accurate enough to be useful in the extra-tropics. Rainfall estimates from SSM/I data may be better, but this has not yet been demonstrated; they have poor global coverage, which also makes validation more difficult.

The two PIPs carried out so far concentrated on the consistency between the many different satellite algorithms. The wide variation in the mean rainfall rates inferred from 25 passive microwave algorithms is displayed in Figure 2.2 for two cases in PIP-2: the first is a continental squall line, the second shows precipitation over the ocean. As seven algorithms are ocean-only, surface rainrates were not computed for those in the land case. This is the reason for the gaps in the histogram in the upper panel of Figure 2.2. The results in Figure 2.2 showing considerable variations among several algorithms and with respect to the validation data. However, Figure 2.3 shows that good agreement is possible when high resolution microwave data from an aircraft overflying a thunderstorm are compared with columnar ice and liquid water contents inferred from high quality ground-based radar data.

2.2.3. What are the Likely Improvements in the Next Few Years?

The work within GPCP will most likely improve the situation in the next years, hopefully going to a $1^\circ \times 1^\circ$ grid with a time resolution of days and for a longer period and based on a larger observational data base. Algorithms for estimating precipitation from passive microwave or infra-red observations from satellites will improve, as should merger algorithms between precipitation analyses from ground-based observations and estimates from satellite observations. This should lead to some improvements in overall accuracy.

Precipitation estimates within analysis/forecasting schemes for weather-forecasts are being increasingly used and operationally compared with observations. This calibration/validation approach should lead to improvements of these estimates.

Operational numerical analysis/forecasting schemes will use observed or estimated precipitation as input and by that provide a better composite estimate of precipitation on a daily basis.

More and improved weather radar networks are being installed although only available over limited areas they are useful for calibration of satellite-based estimates of precipitation.

More vertical profilers may be installed and provide estimates of vertical profiles of precipitation on a continuous basis for a few stations which can be further exploited.

In summary, the likely improvements in the next few years which are listed above are small and will not yield the required data quality. The largest improvement is expected from the TRMM mission planned for launch in 1997. This mission will be described in Section 2.3.

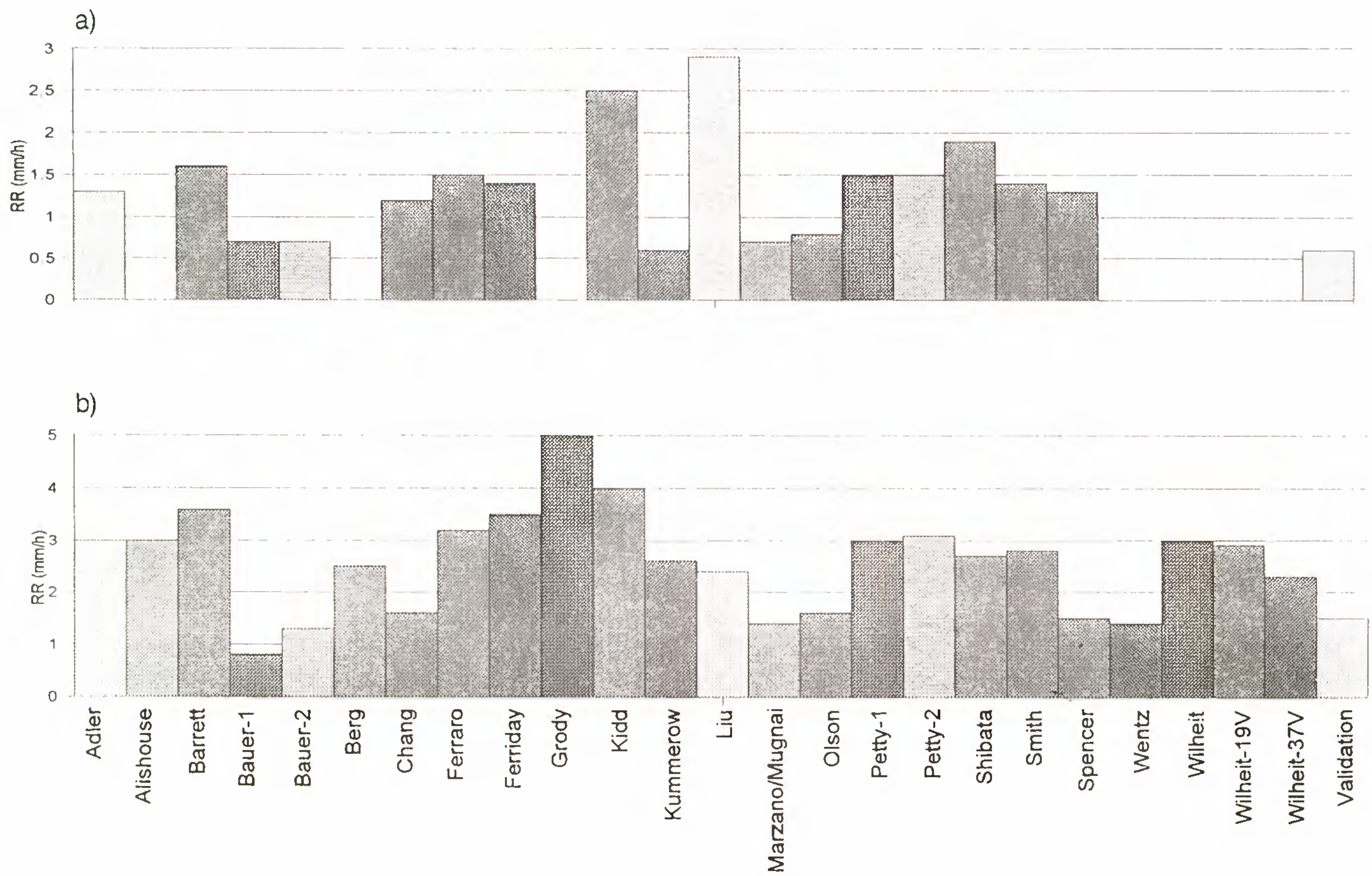

Figure 2.2: *Mean rainrates estimated with 24 passive microwave (23 SSM/I and one MSU: Spencer) algorithms contributing to PIP-2 for two PIP-2 cases: a continental squall line over the southern United States* ***(a)****, and a precipitating system over ocean observed during TOGA-COARE* ***(b)****. Mean rainrates were calculated over the entire target area and are also shown, as a reference, for the available validation data. Note that there are seven ocean-only algorithms, for which surface rainrates were not computed in the land case* ***(a)****. (Adapted from Smith et al., 1995)*

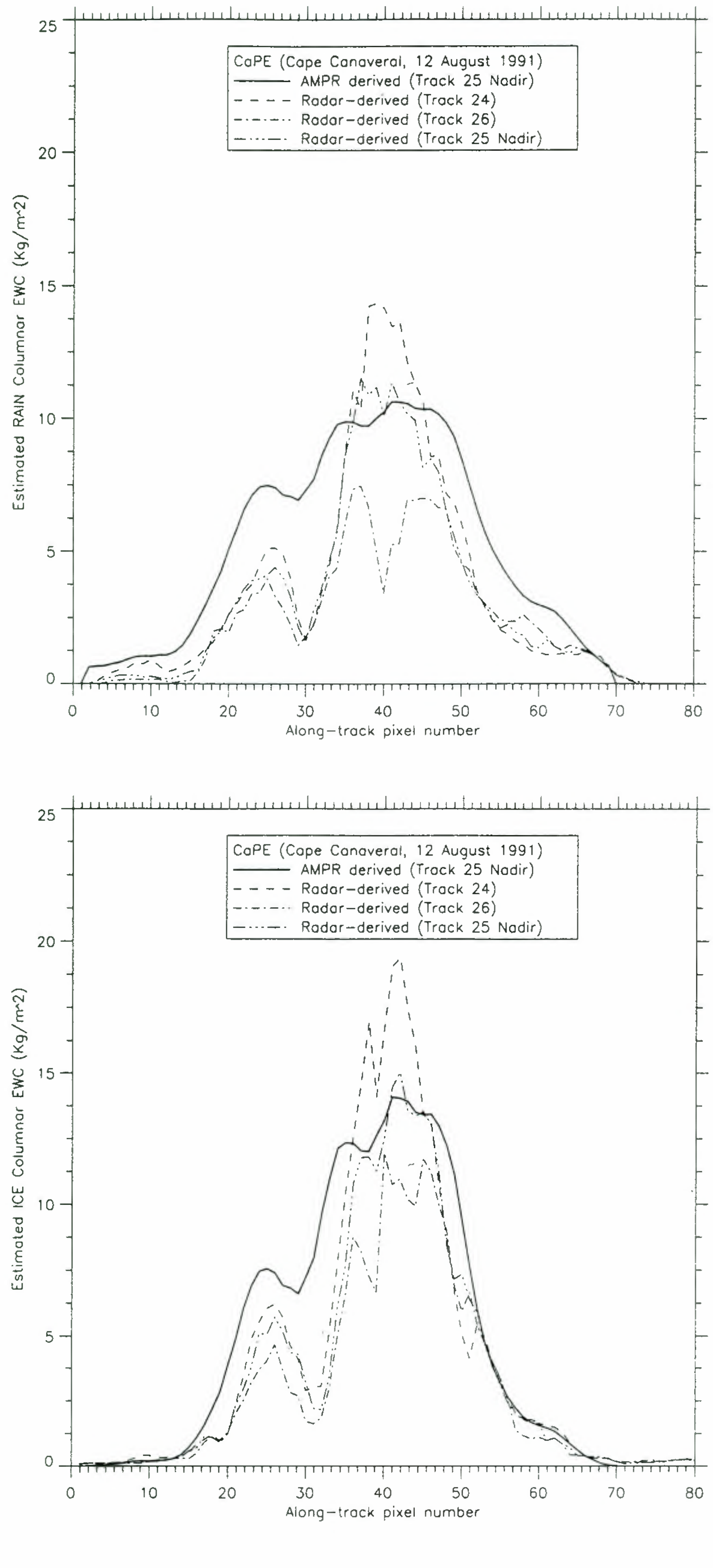

Figure 2.3: *Comparison between rain (top panel) and ice (bottom panel) columnar equivalent water contents (EWCs) estimated from AMPR and CP-2 measurements for a heavy precipitating storm over land observed during CaPE. (Taken from Marzano et al., 1994.)*

2.2.4. Requirements to be Addressed by Satellite Missions

1) More precise climatological means of precipitation for the whole globe on a finer resolution.

   For monthly means one should aim for a $1^\circ \times 1^\circ$ grid and gathered over a longer period and based on a larger observational data base. A higher resolution in time should be aimed for, best for day averages. The daily analysis could perhaps be done on a coarser grid than monthly means.

2) Information on the mean diurnal cycle and its variation through the year is needed.

3) Frequency distributions of number of days with more than several thresholds of precipitation are required. Frequency distributions of drought duration and extremely high rainfall events are needed.

4) Precipitation estimates in polar regions have to be improved.

5) Merger algorithms between precipitation analyses from ground-based observations and estimates from satellite observations or between different estimates from satellite must be improved.

6) SSM/I data have been available since 1987 and many possible algorithms have been proposed to estimate precipitation. There is a need for accurate co-located measurements to test these algorithms.

7) Convective and stratiform precipitation should be separated as numerical models treat the two categories differently. However, there is no unique definition how such a separation is to be achieved in the observations.

8) Distinct vertical profiles of the precipitation should be obtained in the convective and stratiform parts of mesoscale convective complexes (MCCs), and methods to infer the corresponding profiles of latent heat release should be developed. Figure 2.4 reproduces such profiles obtained in an observation of a West African squall line with a ground-based dual Doppler radar system. It should be noted that the heating rate due to latent heat release is much larger than by any other source of heating (e.g. radiation).

9) Observations and estimates of precipitation should be distributed in real time and operational centres should be encouraged to use them for their analysis/forecasting schemes so that a better composite estimate of precipitation on a daily basis can be achieved.

10) Hydrological models need statistics on the variability of precipitation in time and space on very fine scales within a grid or climatologically homogenous area.

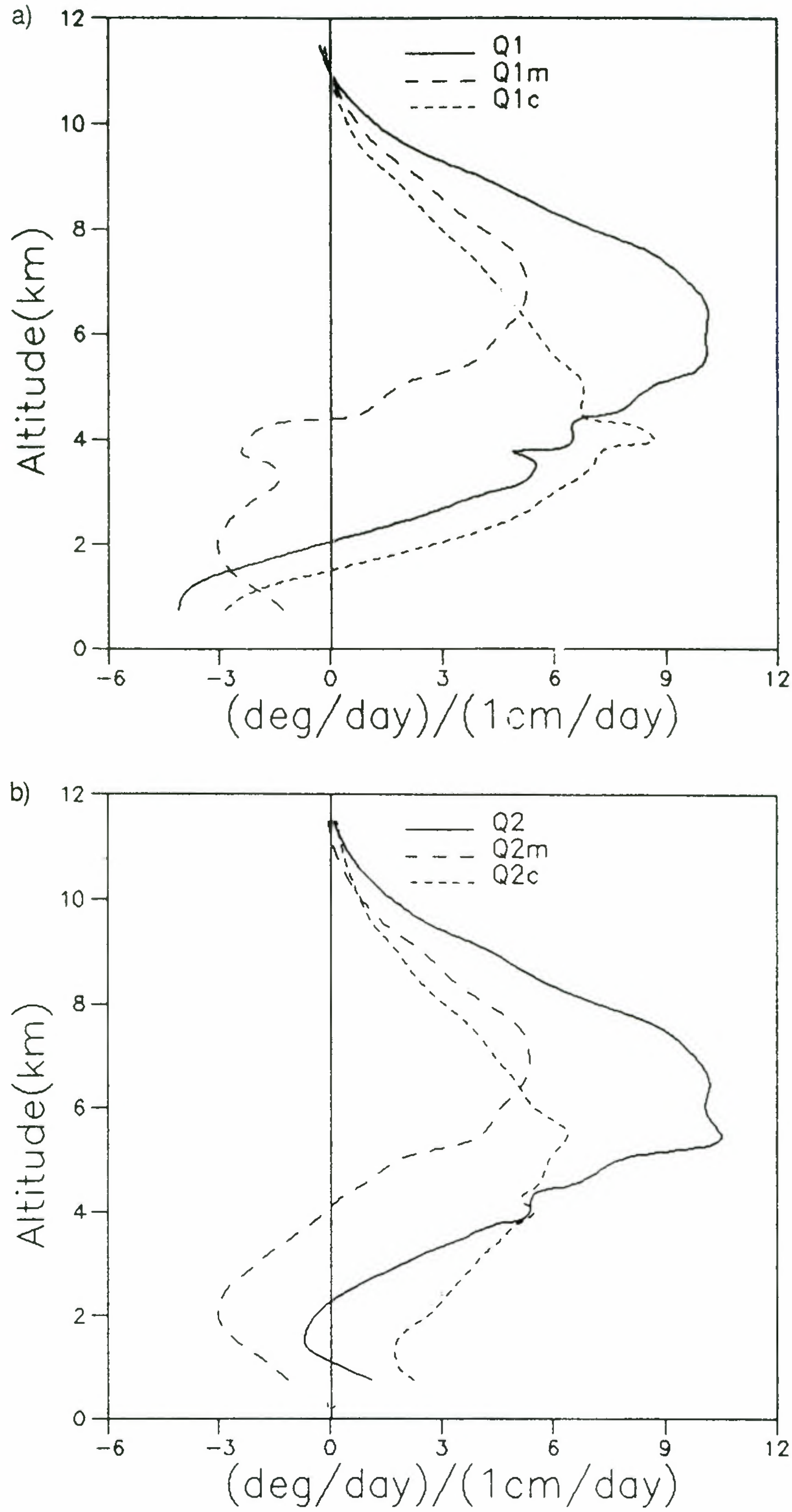

Figure 2.4: (a) *Vertical distribution of the total apparent heat source Q_1, associated with a tropical squall line observed in West Africa, and its partition into sources Q_{1c} and Q_{1m} into convective and stratiform regions, respectively.* ***(b)*** *Same as (a), but for the apparent moisture sink Q_2, and its partition into Q_{2c} and Q_{2m} (from M. Chong and D.Hauser, 1990).*

11) For process studies and case studies it is desirable to get highly precise precipitation values together with a number of other atmospheric fields which are closely related to precipitation, i.e. vertical distributions of water vapour, cloud liquid and frozen water, wind and temperature. Perhaps the ideal environment would be an integration in an observational campaign for the radiation budget.

Figure 2.5 shows for January and July 1987 a north-south cross-section of precipitation averaged between 15° and 25° E as estimated from rain gauge measurements (GPCC), from infrared observations by satellites (GPI) and from two short-range forecasts (re-analysis by ECMWF (ERA) and by the US National Meteorological Centre, NMC). The general distribution is similar in all estimates, as well as the migration of the Innertropical Convergence Zone (ITCZ) over Africa. However, for the ITCZ the GPI estimates twice as much as the ground-based observation. A major uncertainty lies in the positioning of the transition between high tropical precipitation and the adjacent deserts, e.g. in January 1987 at 5° N the values range from 10 to 100 mm/month. In these crucial areas the analyses from gauge observations are especially uncertain because of sparsity of data. For Europe the different estimates agree with an acceptable uncertainty of 20 % in winter (the GPI method is not applicable in extra tropics) while in summer the NMC model values deviate by about a factor of 2 from the others. Although the two best models have been used for the re-analysis and the best estimates from rain gauge measurements have been displayed, the uncertainties in estimates of monthly mean precipitation amounts are clearly demonstrated.

2.2.5. Required Accuracies and Sampling

1) For the purpose of operational weather forecasting, users are more interested in "snapshots" of the precipitation field than in a monthly average. Ideally the resolution of these snapshots should fit that expected to be reached by GCMs within 10 years, namely 30×30 km^2.

2) Within the 30×30 km^2 gridmesh, it is important to separate the respective contributions of stratiform and convective precipitation to the average rainfall rate. Ideally the final product should be the mean profiles of the convective and stratiform precipitation. This should be obtained from the ground to about 15 km altitude, with a vertical resolution of 0.5 km and a relative accuracy of 15 % (or < 1 mm/hour).

3) For monthly means of precipitation at the surface an accuracy of 20 % of the mean or 0.2 mm/day, whichever is greater, for areas of (250 km)^2 should be aimed for. Vertical profiles of monthly means should also be obtained from ground to 15 km altitude with a vertical resolution of 0.5 km and an accuracy of 20 %.

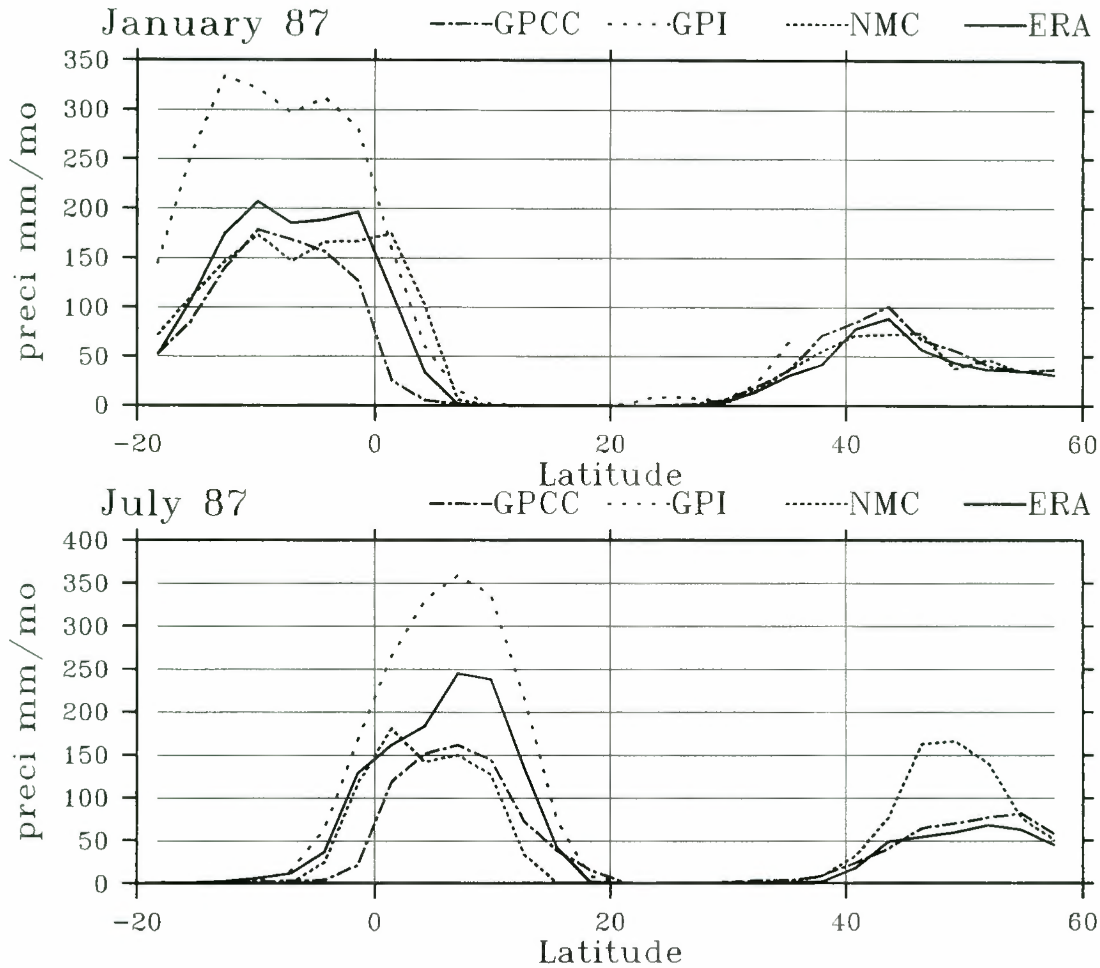

Figure 2.5: *Zonal mean (5° to 25° E) precipitation rate for January and July 1987 for two precipitation estimates (GPCC and GPI) and for two re-analysis products by NMC and ECMWF (ERA).*

4) For the diurnal cycle in long term means: a 3 hour resolution should be aimed for but 6 hourly data would help, the horizontal resolution may be coarse except where there is a sharp gradient in the terrain or vegetation or at the coast. The averaging period could span several years of a calendar month. The accuracy has to be higher than the diurnal cycle itself.

5) The coverage of ± 60°, allowing the survey of mid-latitude oceanic storm tracks, would have a significant impact in the forecast of mid-latitude. In particular the data for North Atlantic storm tracks is important for European forecasts. Also, collection of precipitation data at mid-latitude in the Southern Hemisphere would be valuable for the general validation of GCMs. Therefore an inclination of orbit like 56° is more attractive than the TRMM orbit (35°).

6) The interactive exploitation of the multi-channel microwave radiometer and of the rain radar on the same platform is essential to extend the swath of the instrumental combination.

7) Operational users will require data in real time. i.e. within 2 hours for short range forecasts, 8 hours for the medium range.

8) Variational analysis schemes might prefer to use actually observed quantities instead of derived estimates of precipitation, so the dissemination of original data should be considered.

2.3 Planned TRMM Mission

The tropical Rainfall Measuring Mission (TRMM) is scheduled for launch in 1997 and comprises the following five instruments:

1) Precipitation Radar (PR) at 13.8 GHz, 4.3 km footprint, 220 km swath.
2) Visible/Infrared Scanner (VIRS) 0.6 to 12 μm, 2 km resolution with 720 km swath.
3) TRMM Microwave Imager (TMI) 5 frequencies in the range 10-90 GHz, with 5-45 km footprints, and 680 km swath.
4) Clouds and the Earth's Radiant Energy System (CERES), 0.3 to 50 μm wavelengths, approx 25 km resolution.
5) Lightning Imaging Sensor (LIS) operating at 0.774 μm, 4 km resolution with a 600 km swath.

The TRMM science team (Simpson et al, 1988) identified six priority science questions:

1) What is the four-dimensional structure of latent heating in the tropical atmosphere? How does it vary diurnally, intraseasonally, seasonally and annually?
2) What is the role of latent heat releases in the tropics in both tropical an extra-tropical circulations?
3) What is the relationship between changes in the boundary conditions at the Earth surface (eg sea surface temperature SST, soil properties) and precipitation?
4) What is the diurnal cycle of tropical rainfall and how does it vary in space?
5) What is the relative contribution of convective and stratiform precipitation and how does the ratio vary in different parts of the tropics and in different seasons?
6) How can improved documentation of rainfall improve understanding of the hydrological cycle in the tropics?

The science team states that these questions can be answered in the form of space-time smoothed data sets; a three-year time series of monthly averaged rain rates over 600 km by 600 km boxes (or equivalent) would be extremely valuable for the main scientific purposes. This averaging means that fairly large random errors in individual measurements are tolerable, so long as they are not biased. It also means that the sampling gaps inevitably associated with low Earth-orbiting satellites can be tolerated, provided the statistical properties of rain fields are close to those expected.

The most important instrument for providing the rainfall data is the active range-gated radar which alone can provide vertical profiles of precipitation. In order to provide a 4.3 km footprint, using a reasonable size antenna, a frequency of 14 GHz is used. In addition, the provision of a sensitivity to measure light rain limits the swath width to 220 km. Sampling studies suggest that to provide monthly mean rainfall over 500 km boxes to within 10 % a swath width of 680 km is required.

The TMI passive microwave imager is the second most important instrument on TRMM for measuring rainfall as it can provide the broader swath of 680 km; a key element is the ability of the narrow swath radar to 'train' the broader swath passive microwave imager to provide adequate rainfall data over the broader swath.

The VIRS instrument should provide simultaneous data which may aid interpretation of rainfall from the passive microwave and radar. The CERES instrument is primarily intended to provide better cloud data so the Earth Radiation Budget Experiment (ERBE) can be continued. It should provide top of the atmosphere (TOA) radiation with twice the previous accuracy. LIS will provide an indirect identification of areas of intense convective rain.

The TRMM experiment represents a great advance in that it is the first range-gated radar to be flown in space and should provide the following:

1) Improved estimates of mean monthly rainfall.
2) Data on the vertical profile of precipitation and the consequent latent heat release.
3) Information on the diurnal cycle of precipitation in the tropics.
4) The coincident microwave radiometer and radar data should lead to improved algorithms for precipitation retrieval from microwave radiometers.

While TRMM will provide invaluable data to the user community it will only be a first step and a follow-on mission should be able to capitalise on the information provided by TRMM. In addition, and as indicated in the previous sections, the scientific requirements for the measurement of precipitation lead to complementary data needs which extend beyond the capabilities of TRMM. Most of these needs can only be met by the provision of a dual frequency radar. In particular, the following shortcomings of the TRMM data set – mainly linked to the limitations of a single frequency radar – can be identified:

a) *Attenuation of the 14 GHz radar signal* – attenuation of the 14 GHz radar signal will be severe in heavy tropical rain and must be corrected. Several correction methods for single frequency radar have been proposed, but all of them have shortcomings. One of these is related to the choice of the empirical relationship between attenuation (K) and reflectivity (Z) to perform the correction. Indeed the K-Z relationship is highly variable (due to the variability of the drop size distribution). This is illustrated in Figure 2.6 showing an observed K-Z relationship at 9.3 GHz (derived from the dual beam technique over the TOGA-COARE area), which is very far from that predicted for the Marshall and Palmer "universal" drop size distribution.

Some of the correction methods use the scattering cross section of the surface as a reference target. But again the surface is an imperfect reference, since its backscattering is subject to the surface wind (highly variable below convective rain), and to the impact of raindrops. The dual frequency radar overcomes these difficulties since its algorithm 1) does not processes the surface echo, and 2) automatically adjusts, ray by ray, the K-Z relationship.

b) *Difficulties over land* – proposed single frequency algorithms for the correction of attenuation rely on measuring the return from the ocean surface, which should have a reasonably constant scattering cross section. Such correction algorithms will fail over land. A dual frequency algorithm would have the potential of being used over the oceans and over land.

c) *Sensitivity to drop size distribution* – the relationship between rainfall rate and radar reflectivity of rain is dependent upon an assumed raindrop size distribution. If raindrop spectra are different in different climate zones then calibration presents a major problem and the rainrate algorithms will need climatological tuning. A two frequency radar would provide additional information which would not require climatological tuning.

d) *Uncertainty of the snapshot rain retrieval algorithm* – even if it is assumed that a perfect correction of the radar reflectivity for attenuation has been performed, the rainrate estimate R from the single frequency radar is still subject to the uncertainty of the Z-R relationship due to the variability of the drop size distribution. This uncertainty may easily reach a factor of two in an individual spot measurement. When deriving monthly means, such an uncertainty can be greatly tempered by the averaging process, and by introduction of a "climatologically tuned" Z-R relationship in the analysis. However, the snapshots delivered by the TRMM radar will be not benefit from this noise reduction and will be affected by large uncertainties. With the dual frequency radar, the Z-R relationship (as the K-Z relationship) could be adjusted ray by ray, so less noise is expected even in the snapshots.

e) *Separation of convective and stratiform rain* - to operate the distinction between convective and stratiform rain, several features of the precipitation field may be used. The most obvious is the "bright band" which is the signature of the melting layer in stratiform rain. However, the bright band is not very marked at 14 GHz, and will be difficult to identify when operating at slant incidence (because of the degradation of the radar vertical resolution). The morphology of the precipitation field (small scale deeply convective cells associated with "convective rain", more shallow and horizontally uniform precipitation field characterizing "stratiform rain") is another way to handle the

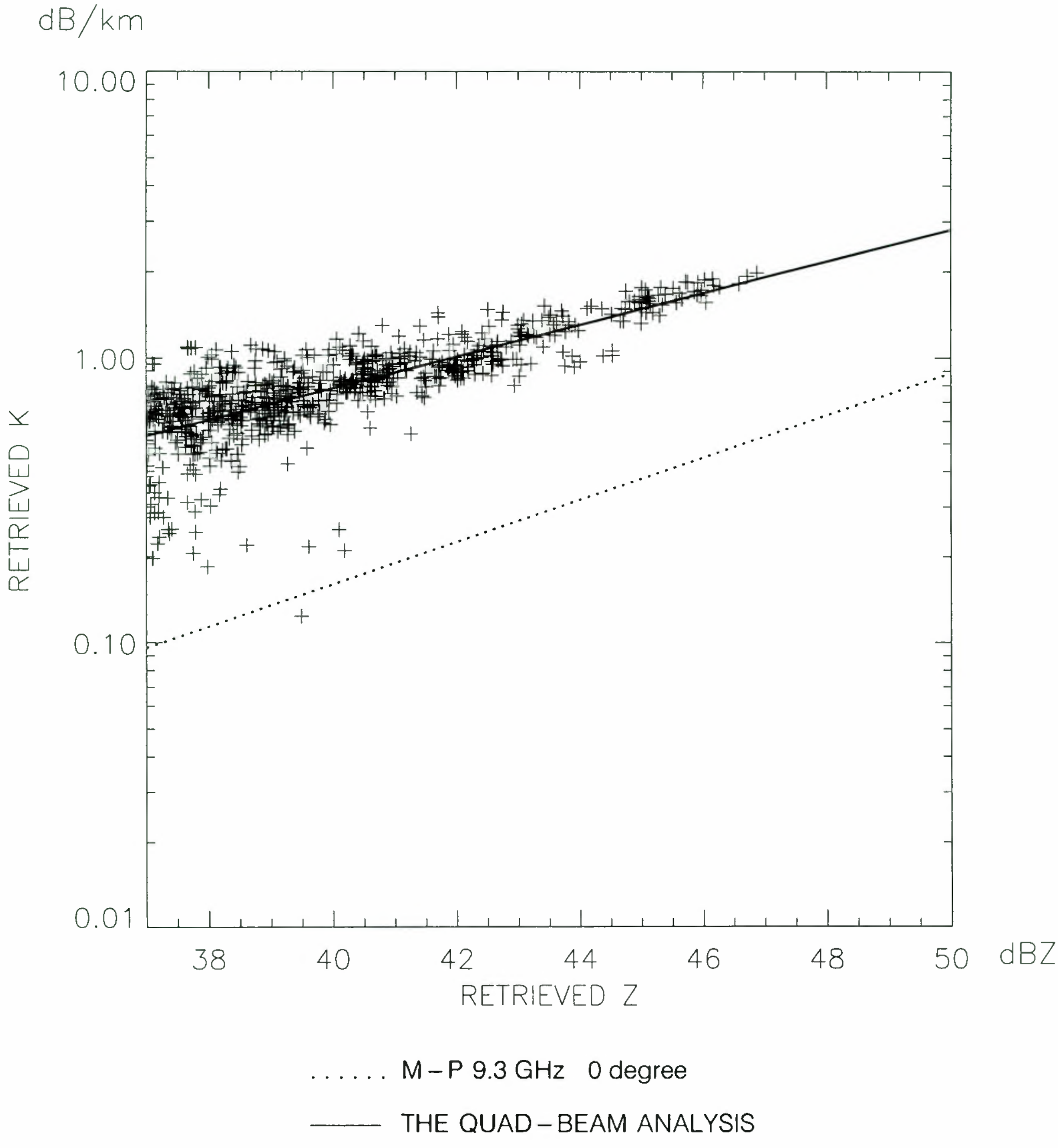

Figure 2.6: *K-Z relationship at 9.3 GHz, derived from the stereoradar technique (Kabèche and Testud, 1995) within a tropical squall line observed during TOGA-COARE with the dual beam airborne radar ELDORA-ASTRAIA. Note that the real data are shifted upward (by more than a factor 2) with respect to the K-Z relation predicted for a Marshall-Palmer drop size distribution, indicating a strong deviation of the real distribution from Marshall-Palmer's.*

problem. The morphology of the transition between ice and rain is indeed determining the separation between convective and stratiform precipitation. A dual frequency radar has the capability to separate ice phase from liquid phase.

f) *Ice and Liquid Water Uncertainty* – the radar returns from ice and an equivalent mass of liquid water are different but the TRMM radar cannot distinguish the two. This introduces an error as the models used for inferring the rainfall rates assume that the targets are raindrops. The TMI radiometer is expected to help in this respect. A dual frequency radar could distinguish different phases.

The other areas where significant improvements could be envisaged are all related to sampling.

a) *Vertical Sampling (i.e. blind layer)* – when operating at slant incidence the meteorological signal at the lowest level is polluted by surface clutter (much more intense) which penetrates through the edge of the main lobe of the radar antenna. This defines a "blind layer" close to the surface, where the meteorological signal cannot be exploited. The blind layer increases with the incidence angle and the antenna footprint. With the TRMM configuration (4.3 km footprint, 350 km altitude), the blind layer depth is more than 2 km at the edge of the swath.

b) *Horizontal Sampling* (i.e. global coverage) – the TRMM instrument only samples the tropics. Although more than 2/3 of global rainfall is believed to fall in the tropics, the remainder is also important.

c) *Temporal Sampling* (i.e. climatological means) – precipitation varies strongly with time on different scales ranging from diurnal to interdecadal. The shortest period acceptable for climatological means is 10 years. TRMM will only provide data for a period of 3 years. However, for unique data sets like e.g. ERBE this criterion has been relaxed.

There are also problems which conceptually cannot be overcome but which it is believed could be improved by the Precipitation Mission. These are:

a) *Swath Broadening* – broadening the 220 km radar swath to the 680 km swath of TMI is vital if monthly rainfall statistics are to be derived. Experiments are now taking place to develop such algorithms. The precise means by which the radar would 'train' the algorithms to be used by the microwave instrument have yet to be implemented.

b) *Sampling* – the studies showing that a 600 km swath from a low Earth orbit satellite can provide monthly rainfall statistics are based on the limited period of radar data in GATE (GARP Atlantic Tropical Experiment). It is not clear that they are universally applicable.

c) *Resolution of the Diurnal Cycle* – it is not clear to what extent a low Earth orbit satellite in a precessing orbit can resolve the diurnal cycle, nor that the poor sampling of the diurnal cycle will not lead to a biasing of the monthly means for a 600 km × 600 km area.

d) *Problem of Latent Heat Release* – the release of latent heat is not measured and models have to be applied to estimate it from profiles of precipitation. It is not obvious how vertical profiles of rainfall rate inferred from radar reflectivity should be converted into profiles of latent heat release required for model validation.

e) *Beamfilling* – the decorrelation distance of rain is comparable with the 4.3 km radar footprint and the 85 GHz microwave footprint. Because radar and radiation signals are not linearly related to rainfall rate, very heavy rainfall cells smaller than the footprint could bias the results; analysis has shown that this is a relatively minor effect.

f) *Hardware Calibration* – calibration of the radar return in terms of a rainfall rate is difficult. Ground-based gauges/radars will usually be unrepresentative of the spatial sample of rainfall made by the satellite.

2.4. Proposed Precipitation Mission

The proposed Precipitation Mission with a dual frequency radar combined with a passive microwave radiometer with a wider swath and improved footprint resolution should capitalise on the TRMM mission. It will have the following features:

1) The use of the dual frequency radar signal which has the following advantages:

   a) It will produce more accurate rainfall measurements than at a single frequency without the need for processing the variable ocean return.

   b) Precipitation products will be available over land and sea with the same accuracy.

   c) Rainfall estimates based on reflectivity estimates have errors because of variable drop size spectra – the dual frequency technique is not affected by changes in drop size spectra.

   d) It can potentially provide real-time precipitation data because the radar algorithm does not require tuning.

   e) It will provide a separation between stratiform and convective precipitation by distinguishing ice from water phase as only liquid water causes attenuation.

2) It will provide data on orographic rainfall.

3) It will have a wider swath for both the radar and the microwave radiometer and so provides better sampling of the rainfall.

4) The data will extend to mid-latitudes, thus improving the understanding of precipitation systems affecting Europe.

5) It will provide better temporal sampling.

6) It will provide more accurate co-located rain-fall data for tuning passive microwave observations for estimating precipitation over land and sea.

7) It will provide statistics of precipitation variability within grid boxes over land.

8) It will complement TRMM by extending the period of observation.

9) It will have a thinner blind layer due to a smaller footprint.

A comparison of the scientific requirements and to which extent they can be met by TRMM and the Precipitation Mission is shown in Table 2.1.

Generally, the mission will:

- help a possible radiation mission to separate liquid water contents into cloud and rain water;
- boost numerical weather forecasting;
- boost model development e.g. parameterization of convection.

Problems which remain to be solved are:

- Models also need vertical profiles of latent heat release while the radar measures vertical profiles of radar reflectivity, the link is not established yet.
- By using passive microwave observations with a swath of 1000 - 1300 km it will be possible to overcome the problem of swath broadening by exploiting the higher accuracy of the dual frequency radar and its ability to discriminate rain from ice.
- Very light precipitation (< 0.3 mm/hour) can hardly be detected by the planned radar.
- For detecting light snowfall over the poles a cloud radar on a polar orbit, anticipated for the radiation mission, might provide some information.

A mission similar to the proposed Precipitation Mission is planned as TRMM follow-on by Japan (see section 7.4).

Requirement	**TRMM**	**Precipitation Mission**
Accuracy of rainfall amounts	reasonable (empirical corrections)	high (two frequencies)
Data availability	over sea	over land and sea
Real-time data	not possible	potentially possible
Distinction stratif/conv precip	difficult	easier
Orographic rainfall data	no	yes
Radar swath	220 km	200 km or 400 km
Microwave radiometer swath	680 km	> 1000 km
Coverage	+/- 30° (tropics only)	+/- 60°
Temporal sampling	poor	improved
Statistics of variability	limited	per grid box
Blind layer at the edge of swath	2 km	1 km

Table 2.1.: *Comparison of TRMM and the Precipitation Mission in respect to the scientific requirements to measure precipitation.*

3. Research Objectives

3.1. Requirements for Precipitation Data

Precipitation is one of the key meteorological variables yet it is one of the most variable in space and time. The detailed representation of the small scale processes involved in precipitation in models of the global circulation is not possible, instead the process must be simplified and represented by a few variables, and the processes parameterised so the precipitation can be simulated by the value of these variables over a grid box which has horizontal dimensions of many kilometres.

Global circulation models of the atmosphere are used both for climate research and for numerical weather prediction. A major activity is the validation of these models so that the parameterisations can be improved. Precipitation data to validate such models is required on a variety of spatial and temporal scales.

The precipitation data at the surface needed for validation is needed at increasing levels of complexity:

1) The simplest validation is to check that the models have the correct values of mean monthly precipitation over a scale of (say) 250 km by 250 km.
2) The next stage is to check that the diurnal cycle of precipitation is being correctly represented.
3) Data is needed to check that the model has the correct variability of precipitation for a given grid box, ranging from the occurrence of droughts to the frequency of extreme flood producing precipitation.
4) Although the tropics are most important energetically, the data is also needed in the mid-latitude and polar regions.
5) Convective and stratiform precipitation is represented differently within models so separation of observations into these two classes is needed.
6) Precipitation plays a crucial role in the vertical transport of latent heat, so vertically resolved profiles of precipitation are required.

3.2. Problems with Existing and Planned Data Sources

Present and planned precipitation data sources all have shortcomings:

1) Ground-based data tend to be point measurements and so suffer from representativity problems. They are sparse in many land areas and almost totally absent over the oceans. They suffer from observational biases especially under snow conditions.

2) Geostationary satellite VIS/IR data provide a measure of cloud top reflectivity and temperature but these are poorly correlated with the underlying rainfall and are confused with thick cirrus. They also fail to detect low level orographic precipitation.
3) Microwave radiometers measure the upwelling radiance at several frequencies which is, in principle, related to the structure of the precipitation, but such is the complexity of the problem that no consensus algorithm has yet been developed. Radiometers fly on satellites in low Earth orbit and so only overfly a given region twice a day at best.

A series of intercomparison projects in which satellite algorithms were compared with ground truth has confirmed the difficulties identified above.

TRMM planned for launch in 1997 will provide the first active rain radar in space with objectives focussed on the tropics. Although it provides a great step forward the following limitations can be identified which should be overcome by the proposed Precipitation Mission:

1) It will operate at 14 GHz. However, this frequency will be attenuated in heavy tropical rain and the data require correction.
2) Proposed correction methods rely on measuring the return from the ocean surface which may be variable, and in any case, is inappropriate for observations over land.
3) Conversion of the derived radar reflectivity into rainfall rate is dependent upon the assumed raindrop size distribution.
4) TRMM will only provide observations over the tropics.

More details can be found in Section 2.3.

3.3. Requirements for the Proposed Precipitation Mission

In view of the unsatisfactory quality of present global rainfall observations the following data are needed:

1) Monthly means of precipitation at the surface are need with an accuracy of 20 % of the mean or 0.2 mm/day whichever is greater, for areas of 250×250 km^2.
2) Vertical profiles of precipitation intensity from the ground to 15 km altitude with a vertical resolution of 0.5 km and a relative accuracy of 15 % (or < 1 mm/hour) for instantaneous values for 30×30 km^2 areas and 20% for monthly means.
3) Discrimination between convective and stratiform rainfall because they are represented differently in the models.
4) Statistics of the time variability of precipitation are needed. For the diurnal cycle 3 hour resolution would be ideal and six hourly useful.
5) Coverage of +/- 60° to cover the mid-latitude oceanic storm tracks.
6) For creating initial fields for operational forecasts, snapshots of precipitation structure with a resolution of 30×30 km^2 in the horizontal, and 0.5 km in the vertical are needed.

Generally, the mission will:

- help a possible radiation mission to separate liquid water contents into cloud and rain water;
- boost numerical weather forecasting;
- boost model development e.g. parameterisation of convection.

4. Observational Requirements

4.1. Sampling

4.1.1. Mission Products

The mission will be essentially based on the association of a multichannel microwave radiometer and of a rain radar. For obvious reasons of antenna footprint, this combination of instruments should necessarily be borne on a low orbiting platform. For such a platform, the revisit time near the equator is in the best case about 11 hours, when a given spot of the surface is within the swath of an ascending and a descending track of the satellite. These constraints provide a guide to define the following two mission products:

1) To produce about twice a day snapshots of the precipitation fields, covering a large part of the globe with a resolution of 30×30 km^2.
2) To provide estimates of monthly averages of the precipitation fields covering the full globe with the resolution of 250×250 km^2 or better.

Concerning item 1, the specification of 30×30 km^2 corresponds to the resolution that is anticipated to be reached by the Global Circulation Models (GCMs) within ten years. It is also a realistic objective from the instrumental viewpoint: the microwave radiometer footprint would be between a few km and about 30 km or less (depending on the frequency channel), while the radar footprint would be a few km (i.e. much more accurate).

In item 2, it is the sampling error which governs the resolution. It has been shown from statistical studies that in order to restrain the sampling error within a 10 % range, the revisit time should not exceed the decorrelation time of the gridmesh-averaged rainfall rate. This decorrelation time is an increasing function of the gridmesh size; the critical value of 11 hours is reached for a gridmesh of about 500×500 km^2. It is clear that such a resolution falls short with respect to what will be achieved by GCMs. A possible way to upgrade the resolution of the mission would be to compensate for the poor sampling by an interactive exploitation with the infrared observations from geostationary satellites and/or taking advantage of likely other passive microwave observations from operational satellites.

4.1.2 Orbit Alternatives

There is an interest of the potential users for improved precipitation data at all latitudes. Observation of precipitation in the tropics is essential because of the role of tropical convection in the dynamics of the global atmosphere. Observation of precipitation at mid-latitude would have an important impact on the weather forecast of developed countries. Observation of precipitation over the polar caps is essential to understand the equilibrium of the polar ice shelf. Thus three options are to be considered and discussed: a polar platform (allowing observations at all latitudes), a mid-latitude platform (with observations restricted to tropics and mid-latitudes), and a tropical platform (focussed on the tropics only) (for illustrations, see Figures 6.6 and 6.7).

Polar Orbit

A low orbiting platform has a period of revolution of about 100 minutes, and covers the globe with about 15 orbits. With a polar platform, the spacing between orbit tracks at the equator is about 2700 km, while the swath of the combined payload microwave radiometer/ radar can hardly exceed 1000 km. So a single platform would only ensure a partial coverage. But the major drawbacks of the polar orbit are:

1) The orbit is fixed (or quasi-fixed) in local time, which biases the statistics of precipitation (subject to a large diurnal variation, at least in the tropics and at mid-latitude).
2) Precipitation over the polar caps is very light, thus the instrument is hardly compatible with that dimensioned to observe tropical or mid-latitude rain which is much more intense.

The light precipitation over the polar caps (mainly in ice phase) could probably be observed independently by a "cloud radar" on another platform.

Tropical Orbit

If the mission is limited to the tropical belt as in TRMM and the same inclination of orbit i.e. 35° is considered, the spacing between orbit tracks at the equator would be 1350 km. This means that with a single platform with an instrument swath of 1350 km (TRMM swath is 680 km), a full coverage of the latitudes within plus or minus 40° with 11-hour revisit time would be obtained. Moreover, the half-period for orbit precession, period of time needed to cover 24-hour local time, would be about 27 days, which is quite favourable to estimate unbiased monthly averages.

Mid-Latitude Orbit

To explore up to a latitude of +/- 60°, an inclination of the orbit of about 56° is needed. But the spacing of the orbit tracks at the equator would then be 2210 km, a swath impossible to be achieved from a single platform. Thus a full coverage with 11-hour revisit time would require two satellites. The half period of orbit precession is about 42 days, which means that 42-day averages should be formed to avoid bias by the diurnal variation (it is acceptable to define "monthly" averages comparable with climate models). With a single satellite, there are the following alternatives: either to optimise the revisit time but accept an incomplete coverage; or to get a complete coverage, but with a revisit time that will largely exceed 11 hours in the tropics. The first choice implies a one-day orbit repetitivity. For the second a two-day or a three-day repetition may be considered.

The one-day orbit repetitivity imposes an altitude of around 500 km. The corresponding coverage of the +/- 60° latitude band, with the microwave radiometer (assuming a 1000 km swath), would be 79 percent. There are holes in the coverage (never visited) below 45° latitude. These holes are large in the tropics. But the band of latitudes 45° to 60° is quite well covered. The coverage with 11 hours revisit time (or better) is obtained at the overlap of ascending and descending orbit swaths. It represents 40 percent of the surface with the radiometer (assuming a 1000 km swath) and 10 percent of the surface with the rain radar (assuming a 400 km swath).

The possible altitudes for a two-day orbit repetitivity are 350 km or 660 km, and for the three day repetitivity, 565 km. The corresponding coverage is 99%, (two-day orbit) or 100 % (three-day orbit), but very few areas are revisited satisfactorily.

Preferred Orbit

The mid-latitude orbit seems the best compromise, for it allows observation of a large portion of the globe (≈ 87% for a 56° orbit inclination), associated with a 24-hour coverage in local time in about 42 days (half period of orbit precession). Concerning orbit repetitivity, the one-day repetition orbit seems more attractive, despite the holes in coverage in the tropics. Indeed such an orbit would allow definition of "calibration sites" which are revisited on average every 11 hours by the platform, that would be helpful:

1) for calibration of algorithms for passive techniques;
2) for comparison with intense field experiments (as for example TOGA-COARE); and
3) for validation of global circulation models.

For the above objectives 1)-3), it is important to collect data at all longitudes. This suggests considering an orbit showing a slow drift of its ascending node. The drift could be chosen in order to accomplish a full geographical revolution within the 5 years of mission duration.

4.2. Radar Technique

4.2.1. The Estimates of Rain from Weather Radar

The basic parameter measured with a ground-based weather radar is the equivalent radar reflectivity factor Z. For spherical raindrops respecting the condition of the Rayleigh scattering i.e. drop diameter $D < 0.07\,\lambda$ (λ: radar wavelength), Z is equal to the integral of the drop size distribution N(D) weighted by D^6. The rainfall rate R is also an integral parameter of the drop size distribution, but weighted by $(\pi/6).D^3.V_t(D)$, where $V_t(D)$ is the terminal fall velocity of a raindrop with diameter D. To establish a relationship between R and Z, the "traditional" approach is to assume that N(D) is an exponential (or a gamma) distribution as

$$N(D) = N_0.\exp(-\Lambda D)\ [m^{-3}\ m^{-1}] \qquad (4.1)$$

and to set the N_0-parameter to the "universal" value of Marshall and Palmer (1948): $N_0 = 0.8 \times 10^7$, $\Lambda = 4100\ R^{-0.21}\ m^{-1}$. In practice, if the assumed exponential (or gamma) shape of N(D) is well verified by natural drop size distributions (as measured by disdrometer or microphysical probe), the N_0 parameter is found to be highly variable (over 2 decades about the "universal" value of 0.8×10^7). This is the traditional difficulty that a classical ground-based weather radar is faced with: any R-estimate derived from Z through a universal Z-R relationship may be in error by 50 % or more.

When operating from space higher frequencies have to be used than in ground-based applications, in order to reduce the size of the radar antenna on the space platform. An additional difficulty has to be addressed: the along path attenuation in rain which means that the radar does not measure Z, but an "apparent" reflectivity Z_a, negatively biased by the attenuation:

$$Z_a = Z - 2 \int K.dr \qquad (4.2)$$

where Z_a and Z are log-reflectivities (in dBZ), and K is the specific attenuation in dB/km.

Thus for a single frequency radar a major issue is the correction of reflectivity for attenuation.

4.2.2. Limitations of a Single Frequency Radar

With a single frequency radar, in any algorithm for correcting attenuation it must be assumed that a K-Z relationship can be well represented by a power law of the form:

$$K = \alpha Z^{\beta} \qquad (4.3)$$

Taking account of (4.3), Equation (4.2) can be solved for Z. However, the solution, first given by Hitchfeld and Bordan (1954) is numerically unstable when the path integrated attenuation (PIA) exceeds about 10 dB. Moreover, the natural variability of N_0 impacts on the K-Z relationship as a variability of the α parameter. Thus, even within its range of numerical stability, the Hitchfeld and Bordan algorithm is sensitive to the uncertainty in N_0.

In the framework of TRMM, many efforts were made to set up improved rain retrieval algorithms from single frequency radar. Most of them use the ocean surface as a reference target, in order to estimate the PIA. This information may be used in two ways:

1) Moderate PIA (i.e. within the stability range of the Bordan Hitchfeld algorithm), may be used to adjust the α parameter of the K-Z relationships (Igushi and Meneghini, 1994).
2) Large PIA can be used as a constraint to stabilize the Hitchfeld and Bordan algorithm (Meneghini and Nakamura, 1990; Marzoug and Amayenc, 1994).

A test of these algorithms could recently be performed from the data of the ARMAR (Airborne Rain-Mapping Radar) 14 GHz radar, an airborne demonstrator of the TRMM radar (on board the NASA/DC8) which flew in TOGA-COARE (see Webster and Lucas, 1992). In particular the application of Igushi and Meneghini algorithm established that the mean value of α during TOGA-COARE was twice as large than that expected from a Marshall-Palmer drop size distribution (Tani and Amayenc, 1995). A comparison of rain rate profiles with various single frequency algorithms has also been performed.

The limits of the single frequency radar may now be appreciated, mainly associated with the variability of the ocean scattering cross section (σ_0), itself subject to the variability of the surface wind (except at 10° incidence which is a neutral point for the response to surface wind), and to the impact of heavy rain. This variability of sigma zero induces an uncertainty of a few dBs in the PIA, with the consequence that:

1) the adjustment of α (of the K-Z relationship) may be performed only on a statistical basis;
2) the 'stabilised' Hitchfeld-Bordan algorithm is subject to relatively large fluctuations.

Moreover, the application of these algorithms over land may be quite problematic because the spatial variability of sigma zero is generally very large (a notable exception: the Amazonian forest where σ_0 is very stable).

4.2.3. Advantage of the Dual Frequency Radar

The dual frequency radar uses the differential attenuation experienced through precipitation by the two probing frequencies. Under the single assumption of the shape of the particle size distribution (exponential or gamma), one may derive from the analysis of the two apparent reflectivities Z_{1a} and Z_{2a} at frequency 1 and 2, the two parameters N_0 and Λ of the distribution, from which any integrated parameter can be derived: the radar reflectivity Z, the specific attenuation K_1 and K_2, the rainfall rate R (Meneghini, Kozu, Kumagai, and Boncyck, 1992). With respect to the single frequency radar, the advantages of the dual frequency for R estimate are two-fold:

1) The variability of the N_0 parameter is taken into account ray by ray (and not statistically as previously);
2) The surface echo does not enter in the analysis; the retrieval is not subject to the natural variability of σ_0; the algorithm performs over land as well as over ocean.

Figure 4.1 displays a comparison of single- and dual-frequency algorithms applied to the data of an airborne radar looking at nadir and operating at 10 and 35 GHz (a joint NASA/NASDA experiment). This figure shows both the importance of correcting the data for attenuation, and the consistency of the retrievals obtained from the various algorithms (with the advantage for the dual-frequency that it does not utilise the surface echo).

An illustration of the improvement brought by the dual frequency radar in the rain rate retrieval is given in Figure 4.2. In this simulation work, it is shown that a variation of the N_0 parameter by a factor 7 affects the dual frequency estimate by less than 10 %, while the single frequency estimate is biased by 40 to 70 % following the algorithm used for retrieval. In terms of bias and standard deviation, the rain estimate from a dual frequency radar represents clearly a progress with respect to the single frequency. Moreover, the dual frequency radar allows estimation of the specific attenuation at any level, which helps discrimination between water and ice (the latter being characterized by about zero attenuation).

In a dual frequency radar, the spacing of the two frequencies should be a compromise between the clarity of the differential attenuation signal, and the overlap of the dynamical ranges at each frequency. Considering the frequency allocation, the two possible choices are 14 and 24 GHz, or 14 and 35 GHz. The dynamical ranges for dual frequency estimate is approximately 2 to 30 mm/hour at 14 and 24 GHz, and 1 to 15 mm/hour at 14 and 35 GHz (covering respectively 68 %, and 57 % of the rain volume in tropical areas). So there is clearly an advantage in the 14 and 24 GHz pair with respect to the 14 and 35 GHz one.

In a dual frequency radar, the ideal configuration is when the two beams scan the same swath simultaneously (ensuring availability of the two frequencies at each spot). With respect to this ideal concept, NASDA considered recently for TRMM follow-on a "degraded" configuration with a cross track scanning radar at 14 GHz, and a nadir pointing radar at 35 GHz. Such a configuration provides the two frequency measurement only at nadir. However it constitutes a clear progress with respect to the single frequency radar since a survey of the variability of the rain drop distributions can be made, and to enable tuning in 'real time' of the K-Z relationships needed in single frequency algorithms. In addition, a 35 GHz radar focussed on nadir could probably detect some non precipitating clouds like cirrus, or ice clouds as anvils related to deep convection.

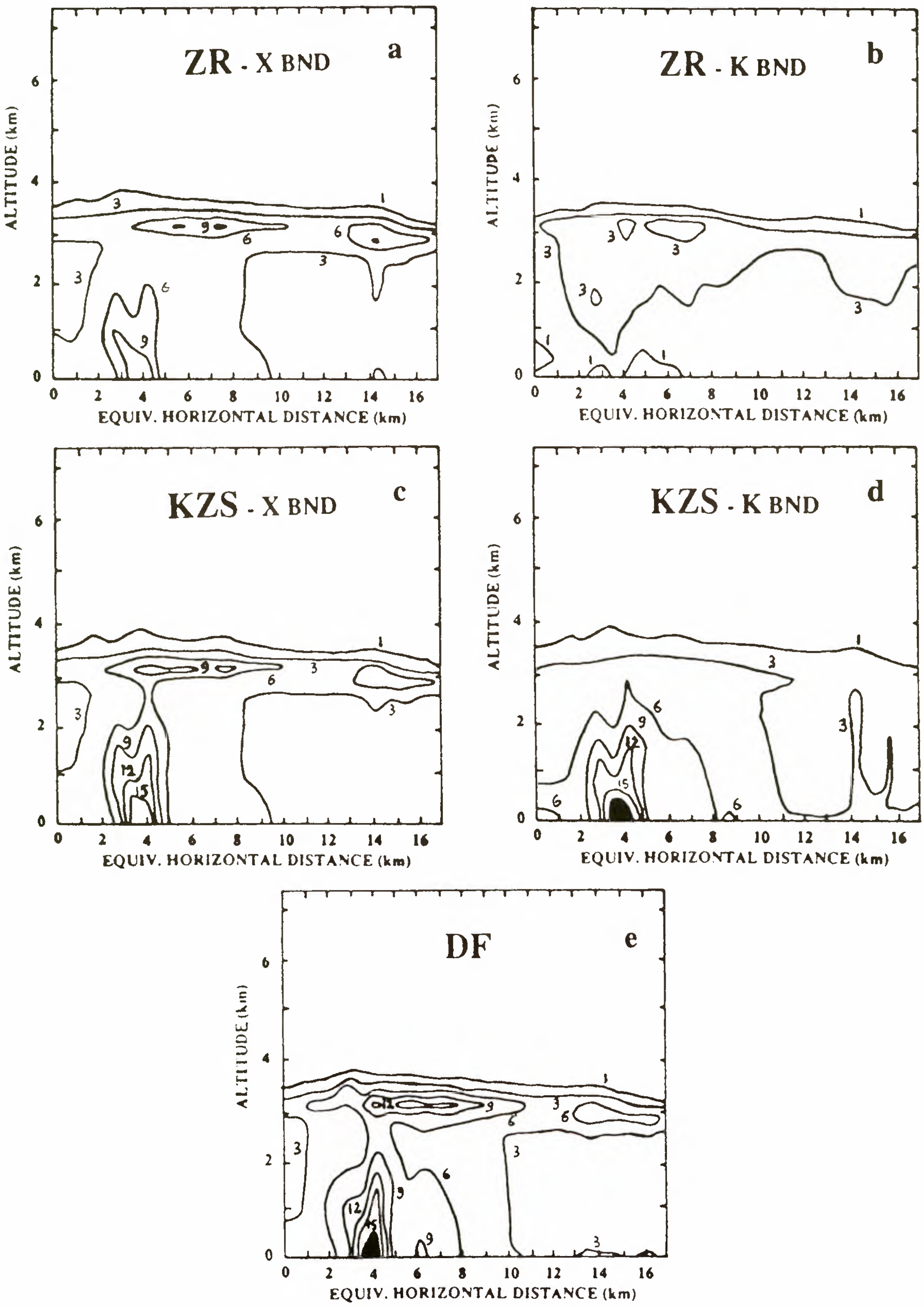

Figure 4.1: *Vertical cross section of rain rate structures reconstructed from the results of various range profiling algorithms: (a) and (b): classical* Z_a*-R algorithm, at X-band and K-band, respectively; (c) and (d): single frequency algorithm with surface echo, at X-band and K-band, respectively; (e): dual frequency algorithm (from Amayenc et al., 1996)*

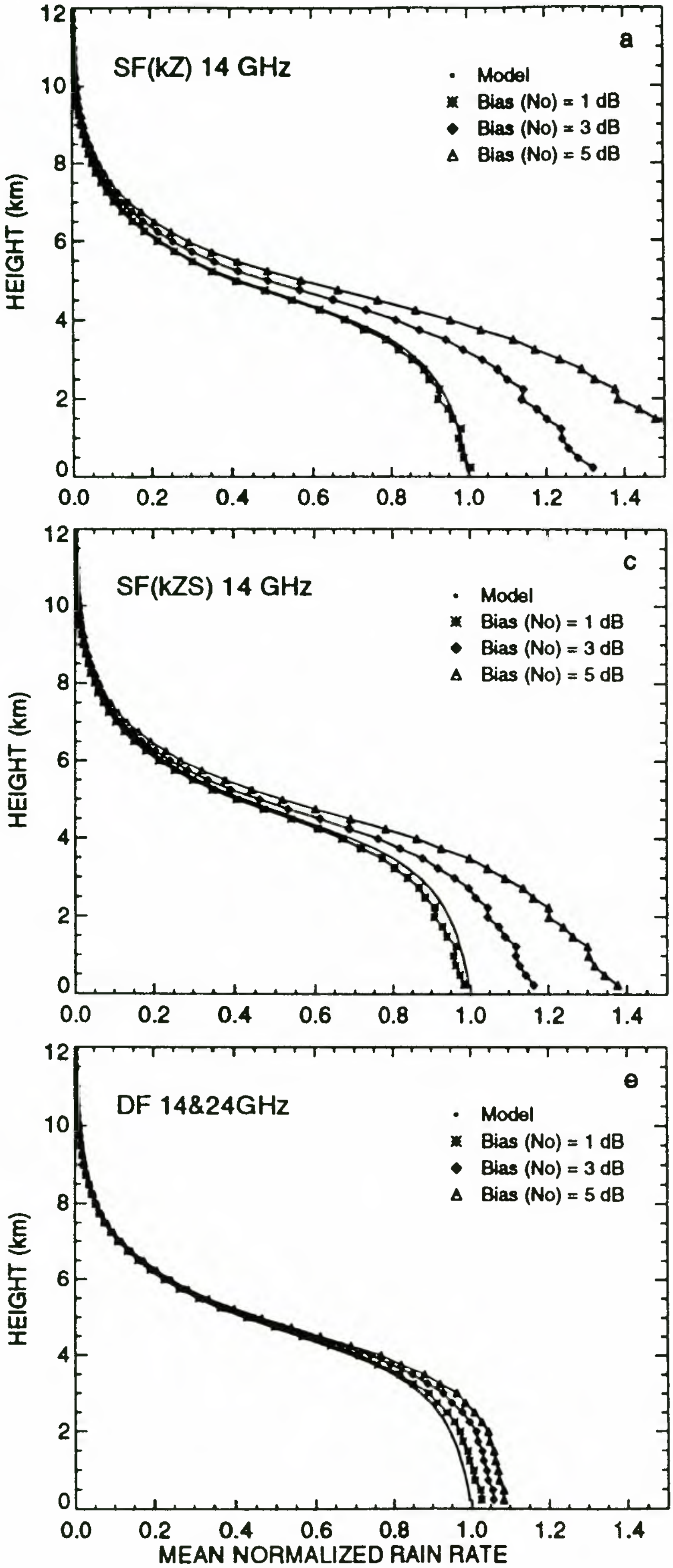

Figure 4.2 : *Comparison of the performances of two single frequency algorithms (upper diagram: without surface echo processing; middle: with surface echo processing) with a dual frequency (lower diagram), in presence of a systematic error in N_0 of 1 dB, 3 dB, and 7 dB (from Amayenc et al., 1996)*

4.2.4. Radar Antenna Footprint

Problems Related to Non-Uniform Beam Filling

One of the difficulties in the measurement of rain is related to its spatial variability. An area of convective precipitation consists of an ensemble of raincells each having typical dimensions of just a few km. Using the statistical observations of Goldhirsh and Musiani (1986), Testud et al (1986) studied the non-uniform beam filling problem, and found that reducing the antenna footprint from 4.3 km (TRMM radar characteristics) to 3 km will lead to some improvements. However, the bias due to non-uniform beam filling becomes unacceptable when the rain rate exceeds 30 mm/hour. This limitation should be accepted and overcome using the statistical approach described in Section 4.5.

Blind Layer Close to the Surface

Another important impact of the antenna footprint on the performance of the rain radar is related to the ability of the system to operate off nadir. At off nadir incidence, the antenna footprint determines: i) the vertical resolution of the measurements, and ii) the ability of the radar to discriminate rain signal from ground clutter, and thus to provide rain measurement close to the surface. The radar footprint, together with the flight altitude, defines the possible swath that the radar may scan without sacrificing too much the vertical resolution and minimum altitude of rain measurements. This is illustrated in Tables 4.1 and 4.2 where it has been assumed that the radar is equipped with an across-track electronically scanning antenna. For two flight altitudes (350 and 500 km) and two footprints at nadir (L = 3 and L = 4 km, one way) both tables show for various distances from the nadir track the pointing angle of the antenna, the vertical resolution (Δh) of the measurement, and the blind layer thickness (h_{min}).

Pointing angle (deg)	Distance to nadir track (km)	Vertical resolution (km)		Blind layer thickness (km)	
		L = 3 km	L = 4 km	L = 3 km	L = 4 km
0.00	0	0.25	0.25	0.125	0.125
5.71	50	0.41	0.50	0.503	0.661
11.31	100	0.71	0.91	0.997	1.325
16.70	150	1.04	1.37	1.52	2.03
21.80	200	1.42	1.87	2.09	2.78

Table 4.1: *Orbit Altitude 500 km*

Pointing angle (deg)	Distance to nadir track (km)	Vertical resolution (km)		Blind layer thickness (km)	
		L = 3 km	L = 4 km	L = 3 km	L = 4 km
0.00	0	0.25	0.25	0.125	0.125
8.13	50	0.52	0.66	0.696	0.92
15.95	100	0.97	1.28	1.416	1.88
23.20	150	1.50	1.98	2.22	2.95
29.74	200	2.10	2.79	3.12	4.16

***Table 4.2:** Orbit Altitude 350 km*

In the tropics, or for midlatitude summer storms, it may be admitted that the data delivered by the rain radar is satisfactory when the blind layer thickness h_{blind} is smaller than 1 km, and then useful when h_{blind} is between 1 and 2 km. For midlatitude winter precipitation, these thresholds should be divided by 2 ($h_{min} \leq 0.5$ km is "satisfactory; 0.5 km < $h_{min} \leq$ 1 km is "useful"). It can be seen that for tropical rain, or midlatitude summer storms, the radar specified in the pre-phase A study (orbit altitude: h_s = 500 km; L = 3 km), referred to as "baseline concept" in the following, means a major improvement with respect to the TRMM radar (h_s = 350 km; L = 4 km): the "satisfactory" swath is ± 100 km about nadir (instead of ± 55 km); the "useful" swath extends to ± 200 km (instead of ± 105 km). However the two other configurations (h_s = 500 km, L= 4 km) or (h_s = 350 km, L= 3 km) are not to be neglected, since they bring the "satisfactory" and "useful" swaths, respectively to ± 75 km, and ± 150 km, an improvement of 50 % with respect to TRMM.

Concerning the vertical resolution Δh, it remains $\Delta h \leq 0.7$ km within the above mentioned "satisfactory" swath, and 0.7 km < $\Delta h \leq 1.4$ km within the "useful" section, which is fully consistent for the description of the precipitation field. However the particular observation of the melting layer (i.e. the ice to water transition layer) requires a resolution of ≈ 0.25 km. This will only be possible at nadir.

Besides its "baseline concept" with electronic scanning, an alternative concept with conical scanning at 14° from nadir, i.e. 15° incidence angle with respect to the surface (antenna footprint is 3 km × 3 km) can also be considered. The performances of the two concepts in terms of vertical resolution and blind layer thickness are compared in Figures 4.3 and 4.4. For reference, these figures also display the corresponding performance of the TRMM radar, and of a ground radar sited on the nadir and operating in the across track direction.

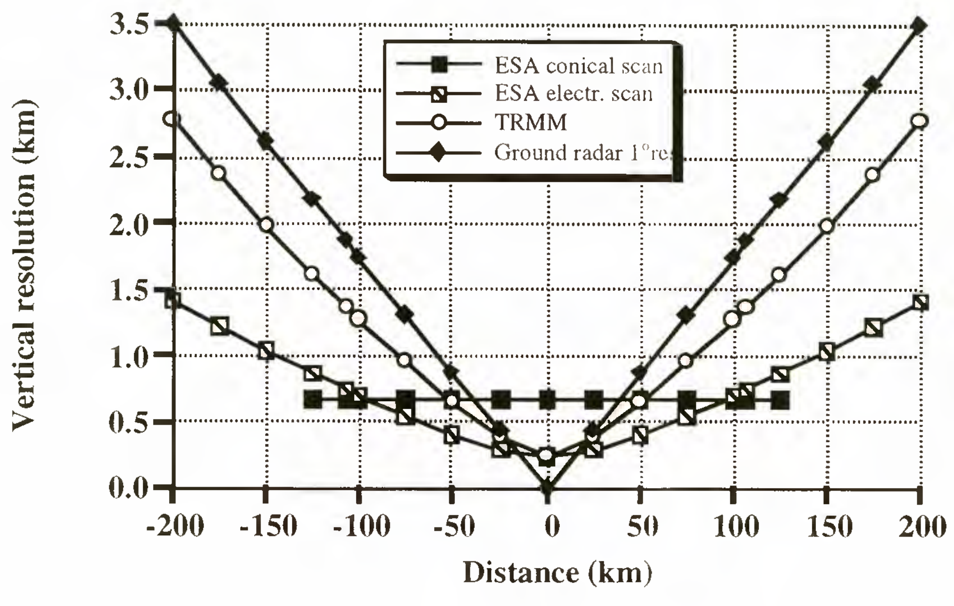

***Figure 4.3**: Vertical resolution, (1) as a function of the distance to nadir track for the three spaceborne concepts (TRMM, baseline - electronic scanning, and conical scanning), and (2) as a function of the range for the ground-based radar.*

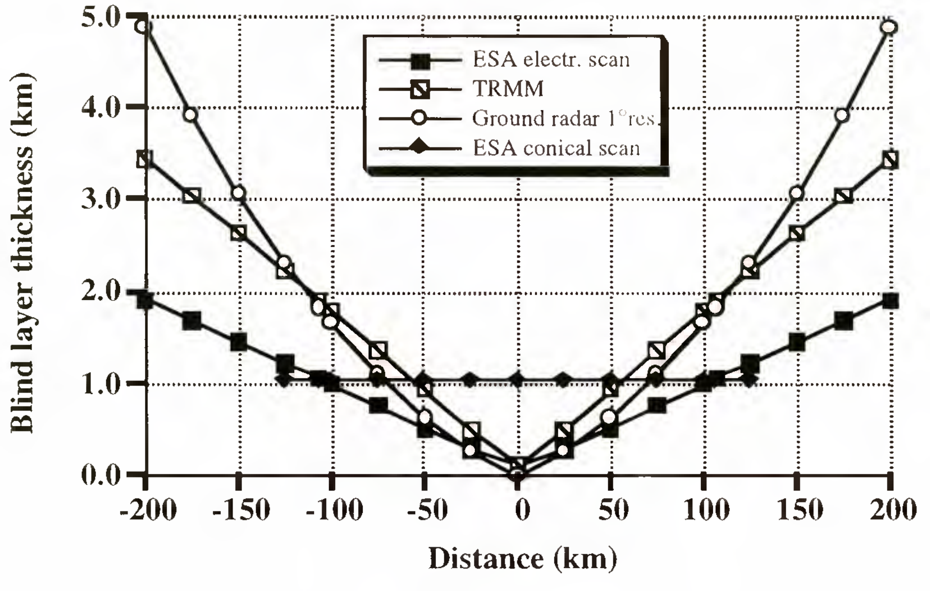

***Figure 4.4:** Blind layer thickness, (1) as a function of the distance to nadir track for the three spaceborne concepts (TRMM, baseline - electronic scanning, and conical scanning), and (2) as a function of the range for the ground-based radar.*

With the conical scanning the radar performance is constant (h_{blind} = 1 km, Δh = 0.7 km) over the full swath covered by the radar (± 125 km about nadir). Meanwhile TRMM gets out of the specification ($h_{min} \leq 1$ km) for distances beyond 50 km, the ground-based radar beyond 75 km, and the baseline beyond 100 km.

4.3. Precipitation Microwave Radiometer

Passive microwave instruments have an inherent flexibility to observe a wide range of multi disciplinary parameters spanning the land, the oceans, the cryosphere and the atmosphere (see ESA, 1996a). This, coupled with their unique ability to obtain observations in almost all weather conditions, day and night, make them of great potential interest to a wide range of users. Combining this powerful observing capability with the global coverage available from spaceborne instruments consequently lead to a widespread interest in passive microwaves, i.e. a precipitation microwave radiometer (PMR).

Precipitation is not the only geophysical parameter that can be retrieved from measurements from a microwave radiometer optimized for precipitation retrieval. The spatial scale of precipitation imposes constraints that normally exceed those from other areas of application.

Channels: Due to the different emissivity characteristics of land and ocean surfaces, the key frequencies for precipitation retrieval over these surfaces also differ. For precipitation retrieval over the ocean the key window frequencies are 89, 36.5, 18.7 and 10.65 GHz. Because the emissivity of land is much higher and spatially variable than that of the ocean, the 10.65 GHz can hardly be used over land. An additional channel in the wing of the water vapour absorption line (23.8 GHz) is necessary to take into account the atmospheric humidity.

Table 4.3 summarises the channels required for precipitation retrieval. Having a 36.5 GHz channel with vertical polarisation in addition might prove useful.

	10.65 GHz	**18.7 GHz**	**23.8 GHz**	**36.5 GHz**	**89 GHz**
CHANNELS	H polarisation	H polarisation	H polarisation	H polarisation	H and V polarisation

Table 4.3: *Requirements for PMR Channels for Precipitation Retrieval*

Spatial Resolution: The relationships between the observed brightness temperatures and the rainfall intensity are highly non-linear. For this reason the average rain rate over a partially filled beam will always be underestimated. The degree of underestimation depends on the actual spatial distribution of precipitation. Only on a statistical ensemble of measurements can this beam filling error be corrected. To minimize this error the beam of the instrument has to have the same scale as the observed precipitation. Since rain is spatially highly variable and has relatively small scales, small foot print sizes are necessary.

Swath: The swath width of the PMR should at least be 1000 km. The objective is to minimise gaps in the global coverage.

Incidence Angle: to ensure consistency with older radiometric datasets (e.g. SSM/I) allowing their extension and possible retrospective calibration; incidence angle with the ground between 50° to 55° (SSM/I is 53°) recommended.

Performance: the radiometric accuracy and sensitivity are not particularly critical in the retrieval of precipitation however, it will be advisable to keep both of them below 1 K.

4.4. Synergy Between Instruments

4.4.1. Synergy between the Precipitation Microwave Radiometer and the Rain Radar

The synergy between the instruments flying on board the Precipitation Mission has two general types of application 1) swath broadening and 2) improved common swath.

Swath Broadening

The radar measurements are limited to a relatively narrow swath while the radiometer has a much wider one. In the narrow swath of the radar high accuracy measurements of the precipitation profile will be possible however these will cover a very limited region of the globe.

The PMR has instead the capability to acquire measurements over a very wide swath (from 1000 to 1250 km depending on the configuration implementation, see Chapter 6) but, when taken only on their own, with a smaller degree of accuracy. This smaller degree of accuracy is due to the variable relationship between brightness temperatures and precipitation that is reflected in climatological or geographical variations of the retrieved precipitation for the same vector of brightness temperatures.

To improve the accuracy, the passive microwave precipitation retrieval algorithm can take advantage (at least) of the information concerning the height of the precipitation layer that can be provided by the radar in the swath area that is common to both instruments.

A higher increase of accuracy of the radiometric precipitation measurements can be achieved by using the data from the radar to 'tune' or calibrate the passive retrieval algorithms. This can be achieved by creating radar datasets that are geographically dependent and then using them to train the passive retrieval algorithm. Under the point of view of the passive remote sensing specialist this technique is not swath broadening (radar point-of-view) but is retrieval algorithm calibration.

Good schemes for this application are those based on passive microwave profile algorithms that use a microphysical generator to produce realistic and detailed profiles of precipitating cloud systems (Smith et al., 1994). The microphysical generators can, in these algorithms, be either cloud-mesoscale models involving explicit microphysics, or multiparameter radar data of observed rainfall systems, or a combination of both. The basic idea is that while the various channels of the space-borne radiometer supply information on the cloud/precipitation structure at different heights above the main precipitation layers, the microphysical generator links these latter layers (and therefore the surface precipitation) to the overlying layers that are sensed by the radiometer. Figure 4.5 shows a block diagram for this type of algorithm where, in this case, the precipitating-cloud database is produced by accurate measurements from the rain radar and will contain not only the information regarding the vertical profiles of the geophysical variables but also the derived brightness temperatures.

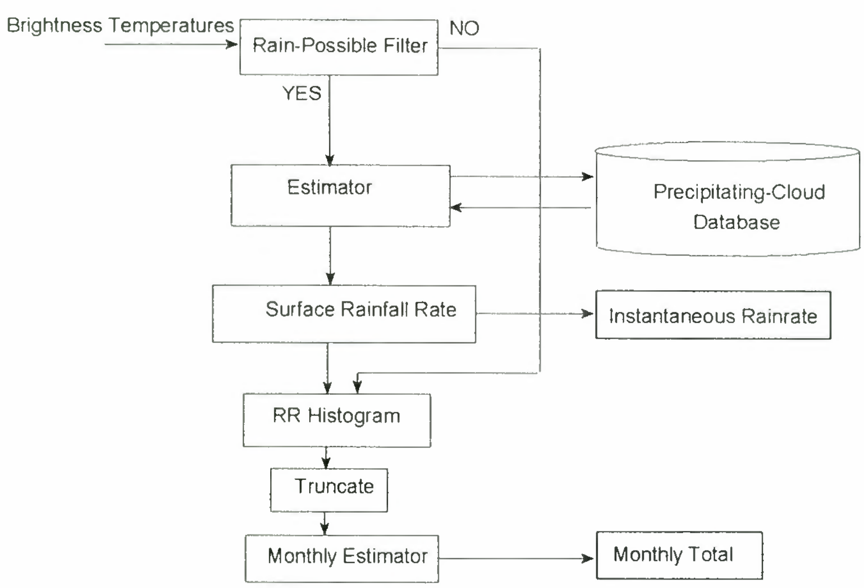

Figure 4.5: *Example of a passive microwave retrieval algorithm that can be used for swath broadening.*

For the specific case of broadening the radar swath of the Precipitation Mission, the database will be generated by the data acquired by the radar and then used by the radiometer. This database should contain, in addition to the usual parameters, information on the geographical location of the data acquired so that only those relative to a specific region are used in the passive retrieval of precipitation for the same region. With this type of technique the accuracy of the precipitation retrieved will be much higher than that achievable when using the radiometric measurements alone and comparable to that performed by the radar, at least for the rain intensity at the surface.

Improved Common Swath

With passive microwave retrieval algorithms, the radar measurements (at least, below the freezing level) can be used together with the radiometric data as an input to the retrieval technique to gain information on the internal structure of the precipitation layer. In essence, while the upwelling microwave radiances (measured by the radiometer) would mainly depend on the depth (i.e., columnar amount) of the precipitation column and not much on its internal structure (i.e., the vertical profile), the radar can detect the structure.

On the other hand, a radiometer-based profile retrieval technique can provide information on the structure of the overlying layers that will be useful to compute the attenuation of the radar signal and therefore improve the radar retrieval. Finally, the radiometer data could be used to provide precipitation structure information in very high precipitation regions, where the radar signal would be too attenuated to be profitably used and/or at the largest radar incidence angles where the radar signal cannot be used to measure low-level precipitation (see Sections 4.6 and 4.2.4). This approach has been attempted with success in the precipitation analyses of coincident airborne nadir measurements taken by NASA's ARMAR (a 14 GHz Doppler radar) and by the AMPR radiometer during TOGA-COARE. It is worth noting that the AMPR-ARMAR configuration simulates the microwave instrumentation that will be aboard the upcoming TRMM spacecraft.

Developing algorithms which make use of both active and passive measurements will help developing better passive microwave algorithms to be used in the extension parts of the radiometer swath which are not observed by the radar.

4.4.2. Synergy with VIS/IR radiometers

Estimates of rainfall by VIS/IR instruments alone are probably inadequate for these purposes, but there are indications that the passive VIS/IR algorithms can provide good rainfall data for regions adjacent to the radar swath, provided that the passive algorithm is optimised for each individual case by the coincident radar coverage.

Although rainfall estimates using only visible and IR data are not reliable, pioneering work by Lovejoy and Austin (1978) using coincident radar and satellite (VIS/IR) data, showed that it was possible to optimise the VIS/IR algorithm if coincident radar data was available so that the optimised VIS/IR algorithm gave very good agreement with the radar. The agreement was good for distinguishing between rain and no/rain, but efforts to produce a third classification differentiating between light and heavy rain were not successful. The optimised rain/no rain VIS/IR algorithm was different in the two regions studied (GATE - West Africa and Montreal) and also changed from day to day. However, as a single optimised algorithm worked consistently over the circle of 180 km surrounding the radar site, it seems reasonable that a satellite VIS/IR algorithm optimised where the radar and VIS/IR swath overlap, could then be extrapolated to regions adjacent to the radar swath where only VIS/IR is available.

Further work by Cheng and Brown (1995) using the extensive UK radar network, has shown that VIS/IR algorithms optimised to match regions where coincident radar data were available, generally provided discrimination between rain and no-rain over an adjoining radar site for cold fronts; for warm fronts and convective events the agreement was much less reliable.

Two limitations of the VIS/IR optimisation method should be emphasised. Firstly, it can only provide an indication of rain/no rain, and not a quantitative rainfall rate. Secondly, it will fail, if the region outside the radar coverage has a different type of rainfall from that within the radar coverage. In addition, all what can be said about the adjacent region is the fractional area containing rain. A method of converting this into an average rainfall rate is needed. Probably VIS/IR from a geostationary imager would be sufficient.

4.5. Extension of the Upper Limit of the Dynamic Range

The upper bound of the dynamical range with the dual frequency algorithm (14 and 24 GHz) is about 30 mm/hour. The single frequency (14 GHz) algorithm is less limited (upper bound is about 100 mm/hour) but it is more and more affected by non-uniform beam filling beyond 30 mm/hour. A bad or incomplete knowledge of the rainfall for rainrates exceeding 30 mm/hour introduces large biases in the estimate of areal integrated rain rate. It is partly to overcome this limitation that the so-called "statistical algorithms" have been conceived (see recent review by Atlas et al., 1995).

The so-called 'area-time integral method' first developed by Doneaud et al. (1981), is based on a statistical relation between the total areal rainfall V and the area where Z exceeds a specific threshold. The coefficient of proportionality depends on the threshold chosen, and should be climatologically tuned. There exists an optimum threshold ensuring the minimum statistical deviation of the relationship.

For the so-called 'multiple thresholding method' (Meneghini and Jones, 1993) it is assumed - well verified experimentally - that the probability distribution function (PDF) of the rain rate is well described by a log-normal distribution. Given a test area, of typically 100×100 km^2, the PDF can be explored between the two bounds of the dynamical range of the radar (between 0.5 to 30 mm/hour typically). By adjusting the parameters of the log-normal distribution to fit the data best, it is possible to estimate the total amount of rain in the test area (including that due to rain rate outside the dynamical range). Figure 4.6 from Meneghini and Jones illustrates an application of the method for various dynamical ranges of the radar. It can be seen than an upper threshold as 20 mm/hour provides quite accurate results.

The thresholding method is relatively easy to implement, and there is no need for climatological tuning. So it seems to be the most appropriate approach to "extend" the dynamics of the radar. It gives reliable results for test areas as small as 30×30 km^2.

Figure 4.6: Scatter plots of the true versus estimated values of area mean rain rates for 37 precipitation maps derived from a ground-based radar, for three dynamic ranges using a log-normal distribution function (from Meneghini and Jones, 1993).

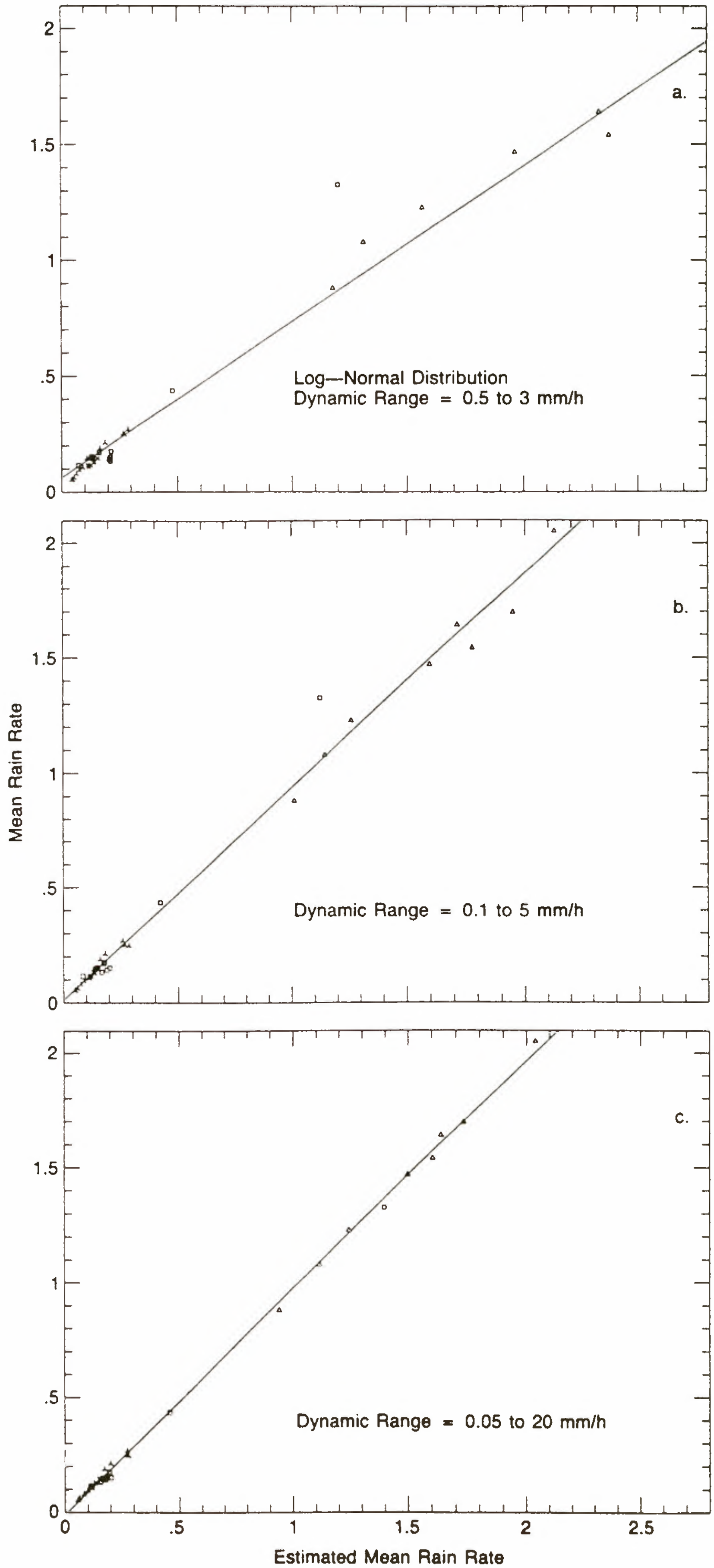

4.6. Exploitation of the Mission in the Absence of Rain

4.6.1. Over Ocean

At the probing frequencies of the rain radar (14 and 24 GHz), the sea surface roughness is mainly due to the surface wind. The scattering cross section of the ocean σ_0 depends on the incidence angle, and on the amplitude and direction of the surface wind. At incidence near nadir, specular scattering is the dominant process while at slant incidence (beyond 20°), σ_0 is essentially due to Bragg scattering. From the Guissard et al. (1992) model, it appears that the transition between "specular" and "Bragg" regimes occurs around 10°, where σ_0 is neutral with respect to the surface wind. Referring to the baseline where the rain radar scans

1) σ_0 is collected at 10° from nadir (the "neutral" incidence), and exploited on a statistical basis, would be used for radar calibration purpose, in particular, to check the stability of electronically across track at ± 22° about nadir, the following exploitation of σ_0 measured in the absence of precipitation could be anticipated: the calibration versus time.
2) σ_0 is collected within ±5°about nadir would be used to estimate the wind speed. Since the radiometric resolution in the σ_0 estimate is expected to be 0.5 dB or less, the subsequent error in the wind speed should be 1 m/s or less.
3) σ_0 is collected beyond ≈15° incidence could also be used to estimate the wind speed. But in addition to the statistical uncertainty of the σ_0 measurement, the unknown wind direction (± 0.5 dB or more) has to be considered, which brings the standard error to about 2 m/s or more.

A conical scanning configuration is more favourable than an across-track linear scan, since conical scanning is the usual strategy in airborne scatterometers. However the incidence angle (15°) considered for the conical scanning rain radar option described in Section 6.7 is rather close to the neutral incidence angle (10°). So the sensitivity of the measured σ_0 to the surface wind will be poor: a dynamical range of 4 dB is expected between weak and strong wind, while in usual scatterometers operating around 30 °, this dynamical range is ≈ 10 dB.

Another possible utilization of the surface wind measurement would be in interaction with the microwave radiometer. With a PMR-type radiometer, in the absence of precipitation, the products of the radiometric inversion are mainly the integrated water vapour content (IWVC), the surface wind speed (SWS), and the integrated cloud water content (ICLWC). Within the ± 50 km swath where the rain radar would provide reliable wind speed measurement, there would be the possibility to validate the radiometer derived SWS (whose standard error is 2 m/s or more). Moreover, using a physical inversion technique (Prigent et al., 1994) to determine IWVC, ICLWC, and SWS, SWS could be constrained to be close to radar derived surface speed (accurate to about 1 m/s), which would help to reduce the uncertainty in the two other parameters (IWVC and ICLWC).

4.6.2 Over Land

The scattering cross section of land surface depends on the soil type and roughness, its humidity, and vegetation cover. The type of radar used for the remote sensing of land surface are high resolution imaging radars operating generally at frequencies lower than 10 GHz (to avoid being perturbed by weather), and at incidence angles larger than 30°. So it is not expected that the rain radar could provide any useful information for this purpose.

On the other hand, the microwave radiometer would be very useful to get information on several land/snow parameters, such as (see ESA, 1996a) vegetation extent, soil moisture, snow cover extent, surface temperature, vegetation biomass, flooding, frozen soil extent, snow liquid water content, and snow characteristics.

4.7 Summary of Observational Requirements

The observational requirements for the Precipitation Mission have been summarised in Table 4.4.

Frequencies (active)	13.8, 24 GHz
Frequencies (passive)	10.65, 18.7, 23.8, 36.5, 89 GHz
Spatial coverage	global (minimum: +/- 60°) with minimum gaps
Vertical range	0.125 - 15 km (at sub-satellite point)
Vertical resolution	250 m (at sub-satellite point)
Blind layer	1 km or less
Horizontal resolution	3 km (at sub-satellite point) (ideally)
Horizontal sampling interval	3 km in both across and along-track directions (ideally)
Rain rate dynamic range	0.3 - 50 mm/hour (at least)
Rain rate measurement accuracy	0.5 mm/hour or 10% whichever is higher
Direct broadcast	desirable

Table 4.4: *Summary of the Observational Requirements for the Precipitation Mission*

5. Mission Elements

5.1. The Precipitation Mission Elements

Reflecting the above requirements of Precipitation Mission observations the following elements are required for the Precipitation Mission in order to fulfil the mission objectives as stated in Chapter 3:

- A dual frequency rain radar (14 and 24 GHz), this would be required to measure vertical precipitation profiles;
- A microwave radiometer, this would be required to expand the swath of the radar; it would also provide, in addition to a passive VIS/IR imager, sensing of surfaces covered by overlaying clouds (ocean, land, low level cloud) and provide, in combination with the radar, liquid and ice water contents (and profiles from synergistic data);
- A GNSS (Global Navigation Satellite System) receiver, this would provide high precision navigation data for geolocation of geophysical products.

Measurements made by VIS/IR imagers and atmospheric vertical sounders might provide useful complementary observations (see Section 5.4).

5.1.1. The Rain Radar

The proposed rain radar would have two frequencies, i.e. 14 and 24 GHz. The swath of the radar would be between 200 and 400 km. The stripes with radar observations crossing the equator would have distances of 2700 km. So there would be gaps of 2400 km without any radar observations at the equator. Further polewards the situation will improve.

5.1.2. The Precipitation Microwave Radiometer

The proposed precipitation microwave radiometer would be a derivative of the Multifrequency Imaging Microwave Radiometer (MIMR) initially proposed for the METOP satellite. Further details on MIMR can be found in ESA (1996a). For fulfilling the scientific objectives of the Precipitation Mission the microwave radiometer would make observations at 10.65, 18.7, 23.8, 36.5, 89 GHz. The minimum swath width would be of the order of 1000 km. The observations with the microwave radiometer will help solving the problem of gaps in coverage at lower latitudes.

5.1.3 The GNSS Receiver for Atmospheric Sounding

The GNSS receiver for atmospheric sounding (GRAS) would provide high precision geolocalisation data for the geophysical products (ESA, 1996b). It would contribute also to temperature and water vapour observations in the troposphere (and lower stratosphere).

However, as this technique provides measurements applying an occultation technique, such measurements would not be available synergetically, i.e. not at the same geolocation as the observations of the other two instruments.

5.2. Satellite and Orbit

The Precipitation Mission satellite is carrying three instruments: a Rain Radar, a MIMR derived precipitation microwave radiometer PMR and a GNSS receiver called GRAS. The satellite is built around a large size Rain Radar. The flying altitude is relatively low –approximately 500 km– and the satellite shape is tailored to minimize aerodynamic forces and torques. Some of its subsystems are conventional but others have uncommon designs due to the required non sun-synchronous orbit. The reference orbit is circular, 24 hours resonant, non sun-synchronous at an altitude around 500 km and with an inclination of 56°. The baselined mission duration is 5 years.

5.3. Ground Segment

The ground segment would consist of a dedicated single ground station at mid-European latitudes and would require a centre for pre-processing the data providing navigated and calibrated but not scientifically processed output and a second centre for producing the scientific outputs. The scientific products would be:

- twice a day snapshots of the precipitation fields,
- monthly averages of the precipitation fields covering the globe with a resolution of 250 km by 250 km.

The whole data reduction process is not time critical (typical delivery times would be 1 to 2 weeks). Data would be provided to users on request. Direct broadcast could be studied as an option during Phase A.

5.4. Supporting Mission Elements

A cloud radar in polar orbit (e.g. on the Earth Explorer Earth Radiation Mission) could provide data on lighter precipitation at the poles. The cloud radar could also provide observations of profiles of ice water content which could be useful for validating precipitation parameterisation schemes in global models used for climate studies and operational forecasting. Visible/infrared data should contribute to the synergy of the radar and microwave retrievals, particularly for swath broadening.

Profiles of temperature and water vapour from operational analysis could aid microwave retrievals and be of assistance in interpretation of radar profiles.

6. System Concept

6.1. General

This chapter presents a baseline concept that has been investigated in two parallel industrial studies on the basis of the identified mission observational requirements. An alternative concept is presented briefly in Section 6.7.

6.2. Payload

The instruments on-board the Precipitation Mission satellite presented in Chapter 5 are discussed in detail hereafter.

6.2.1. The Rain Radar

Instrument Objectives

The objective of the Rain Radar is to provide high resolution measurements of three-dimensional rainfall structure within the volume defined by a radar swath larger than ± 100 km (w.r.t. sub-satellite track) and altitude range of 0 to 15 km, with an additional capability to scan over +/- 200 km at reduced performances. Such information is deduced from the measured radar backscatter signals by rain drops using the method described in Chapter 4. Due to limitations associated with active microwave sensing techniques, the measurement requirements can be met only within a restricted swath width. Depending on the measurement objectives, the radar swath can be extended in order to increase its synergy with the microwave radiometer. Table 6.1 summarises the Rain Radar specifications and Figure 6.1 illustrates the measurement principle. The instrument is a cross-track scanning radar with a single narrow pencil-beam. Some clarification of the requirements are in order:

1) Simultaneous measurements are made at 13.8 and 24 GHz (single-beam, dual-frequency configuration);
2) Both horizontal and vertical resolution requirements are defined at the sub-satellite point;
3) The horizontal resolution is defined by the - 3 dB one-way antenna gain footprint;
4) The lowest measured altitude depends on the cross-track position (scan-angle) and varies from 0.125 to 1000 m (200 km swath) or to 2100 m (400 km swath);
5) Two different swath widths are possible depending on the measurement objectives (200 km or 400 km);
6) The whole rain rate dynamic range is not covered by the radar at both frequencies: the 24 GHz measurement is limited to rain rate not exceeding 20 mm/hour.

The instrument requirements are met – per pixel basis for the case of 200 km swath – with the described design and using an assumed horizontally uniform rain model with the following vertical profile:

Frequencies	13.8 Ghz and 24 GHz
Polarisation	Linear (along or across track)
Mean orbit altitude	500 km
Swath width	200 km (nominal), 400 km (extended)
Vertical range	0.125 - 15 km (at sub-satellite point)
Vertical resolution	250 m (at sub-satellite point)
Horizontal resolution	3 km (at sub-satellite point)
Horizontal sampling interval	3 km in both across and along-track directions
Rain rate dynamic range	0.5-50 mm/hour (13.8 GHz), 0.1 - 20 mm/hour (24 GHz)
Rain rate measurement accuracy	0.5 mm/hour or 10% whichever is higher
Max. range sidelobe level after pulse compression	- 60 dB (w.r.t. compressed peak power)
Measurement modes	1 - Nominal swath 2 - Extended swath 3 - Calibration
Antenna reflector aperture size	6 × 4.8 m
Total instrument mass	370 kg
Total power consumption	340 W

Table 6.1: *Rain Radar Specifications*

$$R_h = \begin{cases} R_0 \; for \; 0 \leq h \leq h_0 \\ R_0 \, 10^{-\left(\frac{h-h_0}{3}\right)} \; for \; h_0 < h \leq h_{max} \\ 0 \; for \; h_{max} < h \end{cases}$$

where: R_0 = rain rate on the ground (mm/hour), h = height (km), h_0 = 5 km, h_{max} = 10 km. Both the specific attenuation and reflectivity are calculated assuming Marshall-Palmer drop size distribution with a water temperature of 10° C.

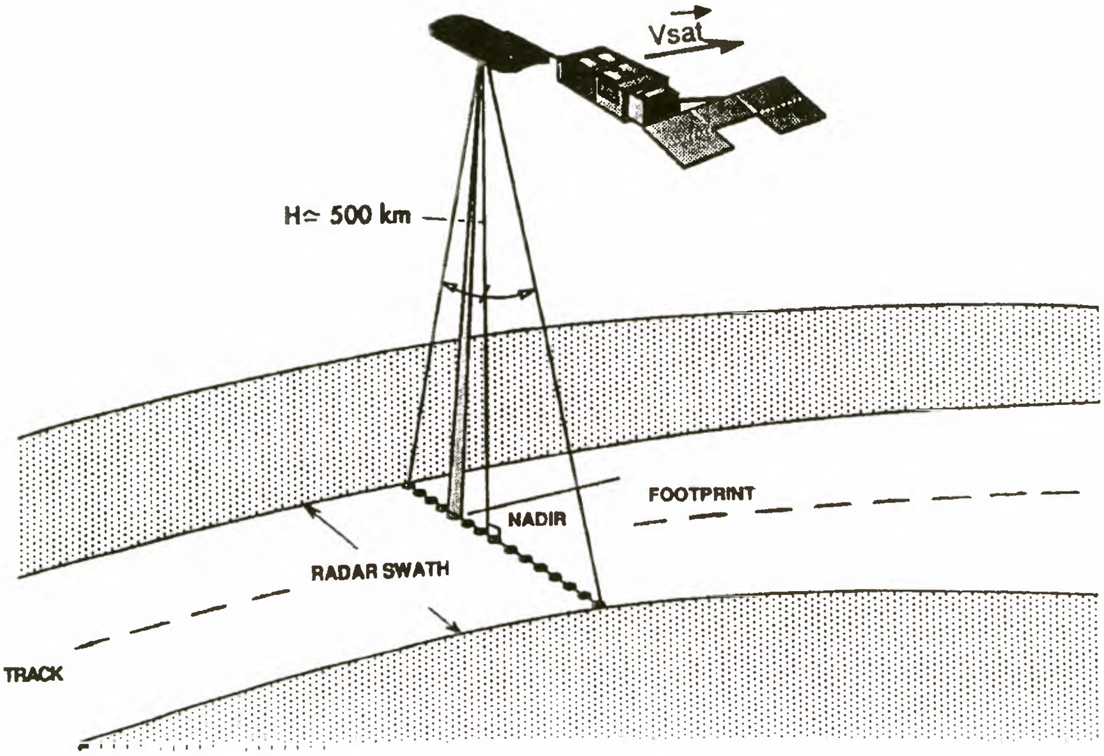

Figure 6.1: *Rain Radar Measurement Principle*

The minimum measured altitude as function of across-track distance can be seen in Table 4.1.

Instrument Description

Figure 6.2 shows the Rain Radar block diagram. The instrument consists of the following subsystems:

1) Digital electronic subsystem which includes the pulse generation unit, the pulse compression unit, the digital processing unit, the time base and the power supply (DC/DC converter). It has digital chirp generation and pulse compression with distortion correction to achieve - 60 dB time sidelobe which is required to control ground clutter.
2) Radio frequency subsystem which includes the RF unit, the power supply and the two power amplifiers (13.8 GHz and 24 GHz).
3) Antenna subsystem which includes 13.8 and 24 GHz feed arrays, the phase shifter controller and a parabolic cylinder reflector.
4) Instrument control subsystem. It provides also the interface with the rest of the satellite.

All subsystems are dual redundant except the antenna subsystem. Redundancy switch matrices assure connections between the subsystems. The reflector is 6 m wide and 4.8 m high. The feed length is dominated by that of the 13.8 GHz feed and is 4.325 m.

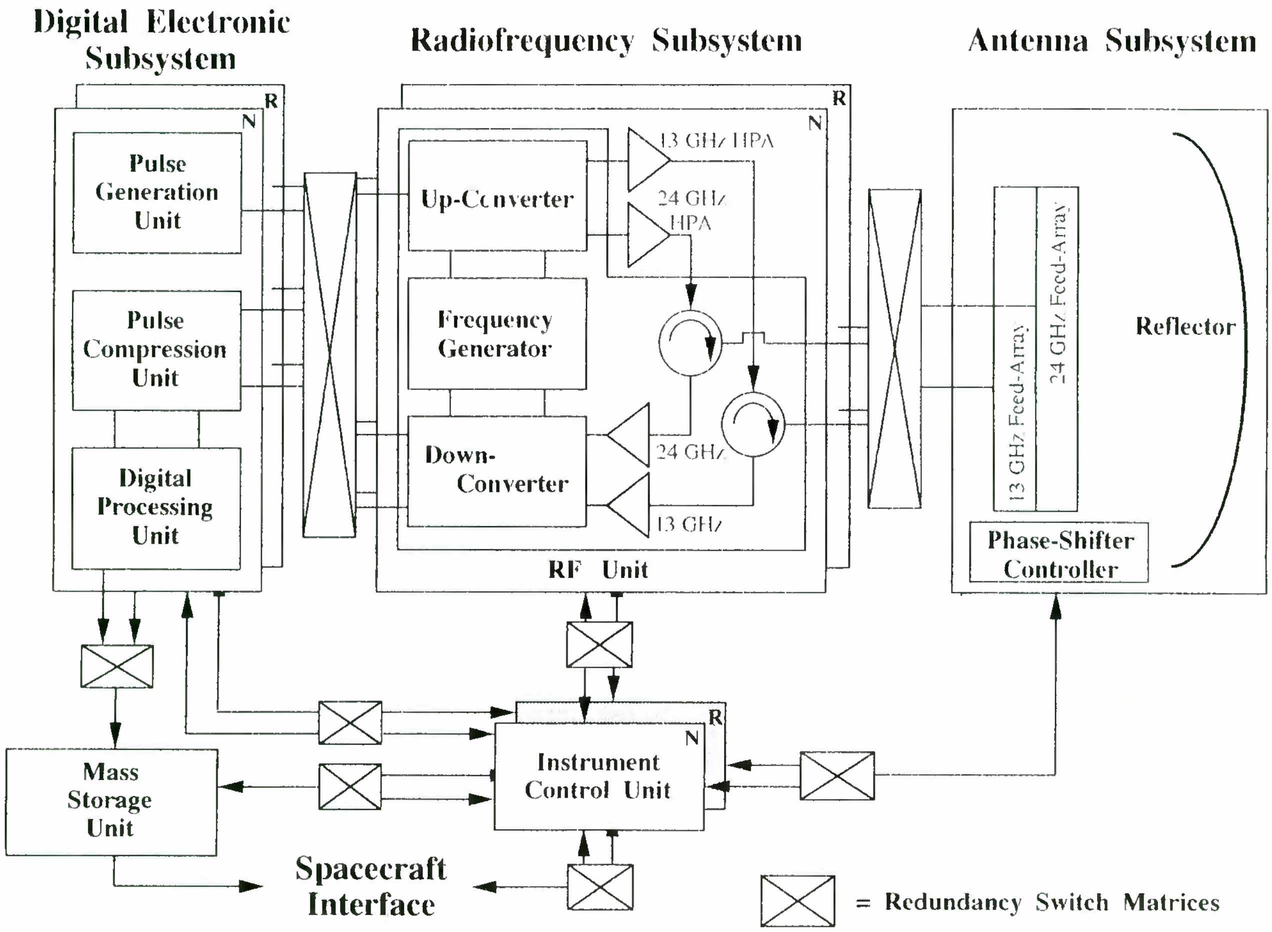

Figure 6.2: *Rain Radar Block Diagram*

The most critical area of the instrument is the large, high precision, dual-frequency electronically scanning reflector antenna subsystem. Specifically, the following requirements must be met (preliminary figures):

1) Better than 0.25 mm RMS surface accuracy.
2) High precision alignment of feed assemblies, reflector (and frequency selective surface if used).
3) Accurate amplitude and phase calibration of the scanning feed assemblies (amplitude < 0.3 dB RMS; phase < 7° RMS).
4) 90% overlap of the 13.8 and 24 GHz antenna footprints (maximum: 6×10^{-4} rad relative pointing error).
5) Peak sidelobe ratio < - 33 dB for all scan positions.
6) Foldability for launch and deployment in orbit.

Instrument Interfaces

Figure 6.3 illustrates the shape and dimensions of the reflector in solid reflector technology and of its feed arrays. In order to ensure a less distorted antenna diagram compliant with required sidelobe levels, an unobstructed antenna aperture must be maintained. In this respect, the complete antenna assembly must be mounted as far away as possible from the platform. Table 6.2 below summarises the dimensions of the feed assemblies. Each of the feed assemblies comprises 272 horn radiators.

Feed spacing	15.9 mm (13.8 GHz)	9 mm (24 GHz)
Feed height	43.7 mm (13.8 GHz)	44.7 mm (24 GHz)
Feed depth	125 mm	
Total feed length	4.325 m (13.8 GHz)	2.448 m (24 GHz)

Table 6.2: *Main Dimensions of the Feeds*

Reflector total mass	145 kg
Feed assemblies total mass	80 kg
Internal subtotal total mass	82 kg
Other (e.g. harness, contingency)	63 kg
Grand Total	370 kg

Table 6.3: *The Mass Budget of the Rain Radar*

The total power consumption is 340 W.

The data rates are: 450 kbit/s for a 200 km swath and 700 kbit/s for a 400 km swath.

Instrument Development Status

Two industrial Pre-Phase A system level studies have been completed in 1995. A pulse generation and compression subsystem has been breadboarded which meets the less than - 60 dB range sidelobe requirement. The subsystem comprises digital chirp generation and pulse compression with a waveform correction to compensate for distortions introduced in the radar transmit and receive chains. The high range sidelobe attenuation is achieved by means of a broken linear FM modulation of the transmit pulse which enables robust control of the range sidelobes in the presence of signal Doppler spread.

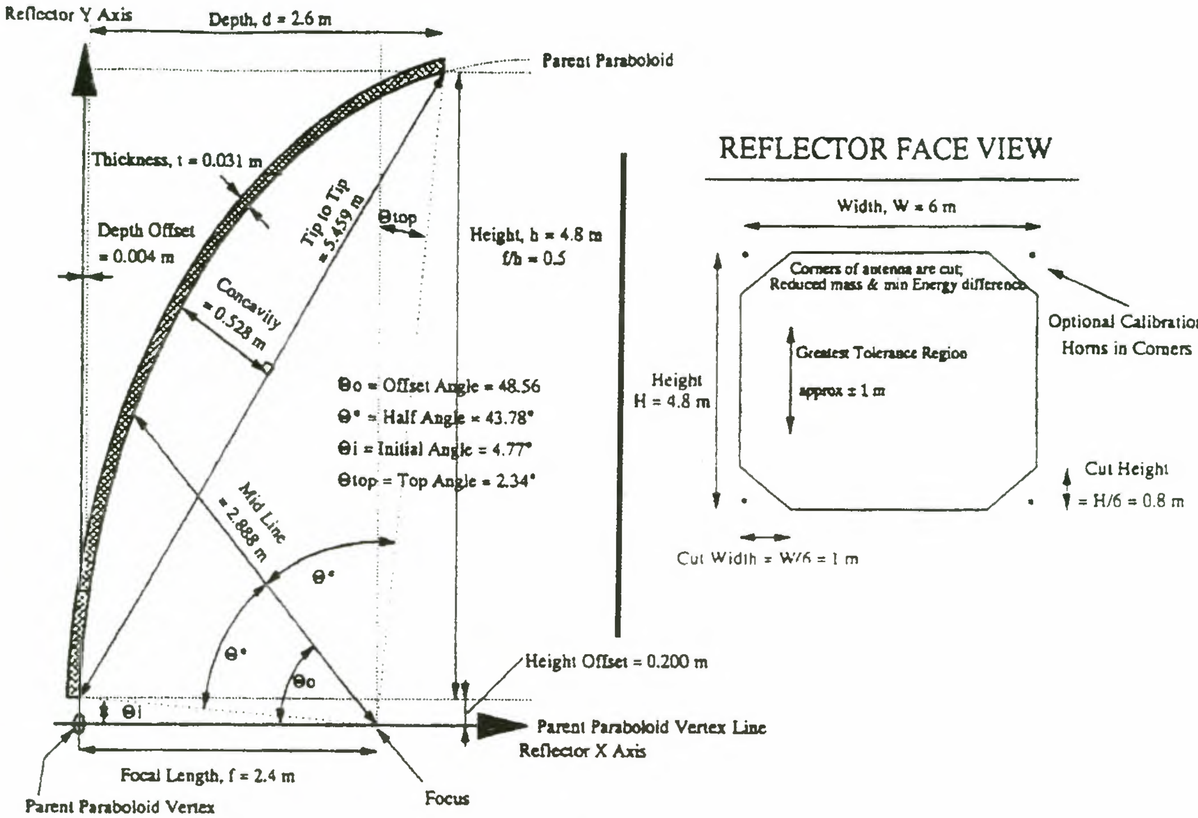

Figure 6.3: *Shape and Dimensions for Solid Reflector*

6.2.2. The Precipitation Microwave Radiometer

For the selection of the radiometer payload it is proposed to benefit from ESA's experience gained during the development of the MIMR demonstrator. The proposed baseline for the precipitation microwave radiometer is a MIMR derivative called PMR as explained below.

MIMR Description

MIMR is an ESA development of a conically scanned radiometer with a scene scan angle of $\pm 60^\circ$ in azimuth. For the MIMR nominal satellite altitude of 800 km, this scan angle corresponds to a swath of about 1600 km providing 82% coverage of the Earth in 1 day from sun synchronous orbit. The radiometer spins about the local spacecraft vertical at 26 rpm with its boresight pointed to obtain an incidence angle of 55° on the ground (see Figure 6.4). MIMR uses 6 frequency bands (6.8, 10.65, 18.7, 23.8, 36.5 and 89 GHz) in the two (horizontal and vertical) polarisations. The corresponding receivers are total power radiometers externally calibrated at every scan rotation by a cold space mirror and an artificial hot target. The main reflector consists of an offset parabola 1.6 m $\times$ 1.4 m in size which is illuminated by 10 feed horns arranged as close as possible to the focal point.

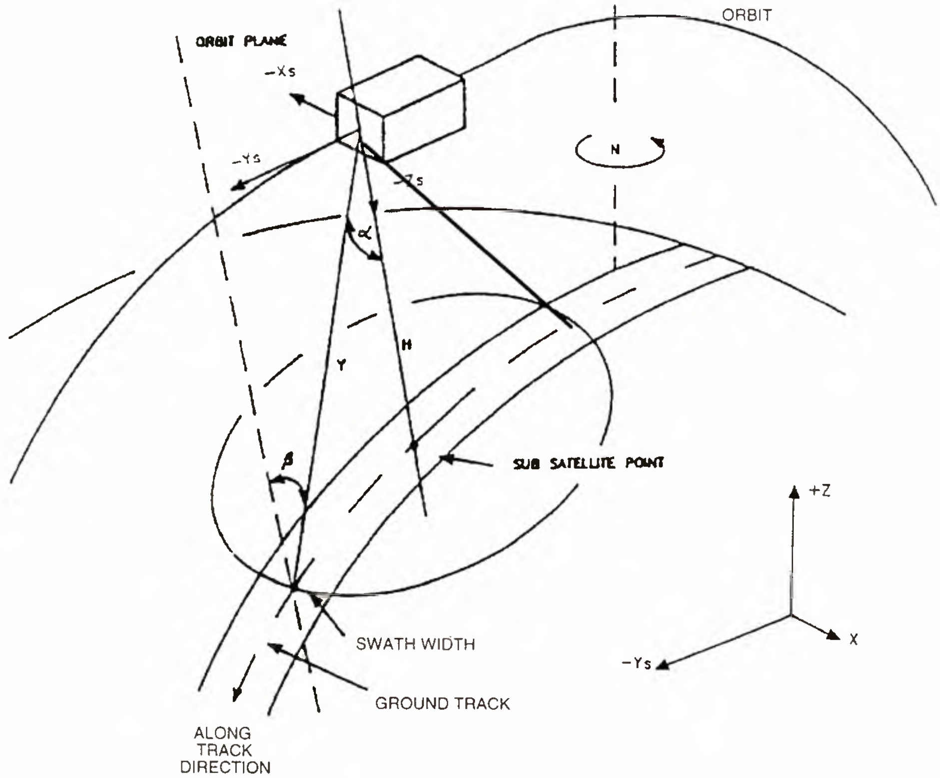

Figure 6.4: *Scan Geometry of the Multifrequency Imaging Microwave Radiometer*

Main reflector, feeders and receivers are all mounted on the spinning drum, together with the digital data, mechanical balancing and associated power subsystems. The scan of the drum is matched to the orbital velocity to provide continuous sampling across scan. Continuous coverage across scan is achieved even for the two highest frequency channels by using the whiskbroom technique (multiple beams across scan). The drum rotates about a shaft fixed to the platform to which the cold mirror and hot load are attached. All data and power signals pass between the drum and the platform through a roll ring assembly.

A derivation of MIMR into a baseline for the PMR has to be performed on the basis of the requirements coming from the combined operation with the rain radar. Major differences with respect to MIMR baseline concern the use of only those frequency channels relevant for precipitation, the orbital height and inclination. Among the frequency channels of MIMR the lowest one (6.8 GHz) does not provide any significant information on precipitation. It is therefore not retained for PMR. The reduction in altitude will improve the radiometric resolution of the basic MIMR but the rotation rate has to be increased.

The PMR will be a total power conically scanned radiometer which measures in 5 frequency bands (10.65, 18.7, 23.8, 36.5, and 89 GHz). 89 GHz (and possibly also 36.5 Ghz) would be sensitive to two polarisations (vertical and horizontal). The reflector size (1.6 m × .4 m parabolic offset) would be as in MIMR. The across and along scan spatial resolutions of the highest frequency channel match rather well the rain radar footprints at the orbital height.

The main requirements can be seen below:

Nominal altitude (km)	500				
Frequencies (GHz)	10.65	18.7	23.8	36.5	89
Polarisation	H	H	H	H (+V)	H+V
Incidence angle (°)	55				
Azimuth scan angle (°)	±60				
Across scan footprint (km)	30	17	14	8.9	3.6
Along scan footprint (km)	17	10	7.8	5.1	2.1
Spinning rate (rpm)	32				
Footprint overlapping (%)	60	29	10	31	15
Bandwidth (MHz)	100	200	400	1000	6000
Radiometric resolution (K)	0.8	0.9	0.7	0.6	1
Swath width (km)	1050				

Table 6.4: *The Precipitation Microwave Radiometer (PMR) Specifications*

Instrument Interfaces

The following interface data are from MIMR, due to the similarity of concepts they can provide a good reference for PMR. The instrument is actually designed to have a rotating sensor assembly (containing antenna subsystem, electronics, mechanisms, thermal hardware, etc.) with a release devices subsystem externally mounted onto the satellite and a set of equipment (mainly electronics and harness) integrated inside the platform. The rotating sensor assembly is continuously scanning in operating condition. The overall dimensions (without thermal hardware) are given in Figure 6.5.

Elements which have field of view requirements for instrument operation are: antenna reflector and feeds and the cold calibration mirror. The mass of MIMR is estimated to be about 200 kg.

Current power consumption of MIMR in nominal operating condition is 200 W including 15% contingency. Data rate of MIMR is 150 kbit/s.

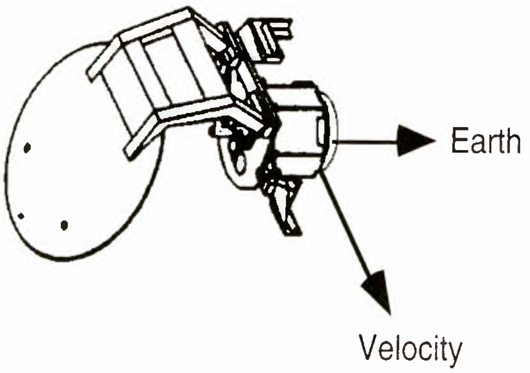

Figure 6.5: *General View of the PMR*

Instrument Development Status

The MIMR instrument has already undergone a development phase up to a complete Phase B. In addition, in the context of the METOP preparatory programme, the breadboarding of an integrated instrument demonstrator including all most significant or critical components is being performed

6.2.3. GRAS

GRAS is a GPS/GLONASS receiver with geodetic quality, i.e. it provides measurements at two frequencies (for ionospheric corrections to be feasible) with random noise in the signal carrier phase measurements below 1 mm, as required for precise positioning and atmospheric sounding. It has been in development by ESA during the last 3 years. The receiver architecture is also compatible with on-board operational utilization as a real-time position sensor is also flexible with respect to the selection of the signals to be tracked (any arbitrary combination of GPS and GLONASS signals). More information can be seen in the description of the Atmospheric Profiling Explorer. The main interface characteristics of GRAS are the following:

Mass (kg)	Power (W)	Data Rate (kbps)	Volume (m)	Accuracy (mm)
3	20	10-20	$0.3 \times 0.06 \times 0.2$	1

Table 6.5: *The Main Interface Characteristics of GRAS*

This instruments has a double purpose:

- It provides autonomous position to geolocalize measurements.
- It contributes to atmospheric temperature and humidity soundings each time a GPS or GLONASS satellites raises or sets behind the horizon.

For autonomous position and velocity determination, an antenna looking in the Zenith direction is needed. For atmospheric profiling a flat patched antenna will be limb pointing and looking in the anti-velocity direction. The key figures of the antennas are:

	Volume (m)	Mass (kg)
Helix Antenna	$0.1 \times 0.1 \times 0.3$	3
Flat Antenna	$0.7 \times 0.7 \times 0.05$	5

Table 6.6: *The Main Characteristics of the GRAS Antennas*

6.3. Mission and Operations Profile

The possible orbits have been compared in Chapter 4. The currently selected orbit is:

- circular,
- at an altitude of 500 km,
- with an inclination of 56°, and
- a repeat time of 24 hours and 15 orbits.

With a 24 hours repeat time it provides an average revisit time of 11 hours. A repeat time of 24 hours is achieved with 16 orbits at 200 km altitude. At that altitude aerodynamic drag is too high and the swath of the instruments will be very small. A repeat time of 24 hours is achieved with 18 orbits at 800 km altitude. At that altitude the Rain Radar will require excessive power and dimensions. The chosen repeat time of 24 hours and 15 orbits appears the optimum solution. The coverage patterns for both instruments can be seen in Figures 6.6 and 6.7. Also the effect of swath widening of the radiometer can be appreciated by comparing both figures.

The inclination is a compromise between the need to have quick local time drift – to avoid biases in the statistics of precipitation – and the need to cover not only the tropics but also the mid latitudes. With 56° inclination, the half period local time precession is 42 days.

The main disadvantage of the selected orbit is that it does not cover completely the accessible Earth. For a 1000 km microwave radiometer the percentage covered is 79 %; nevertheless the coverage at European mid-latitudes is almost total.

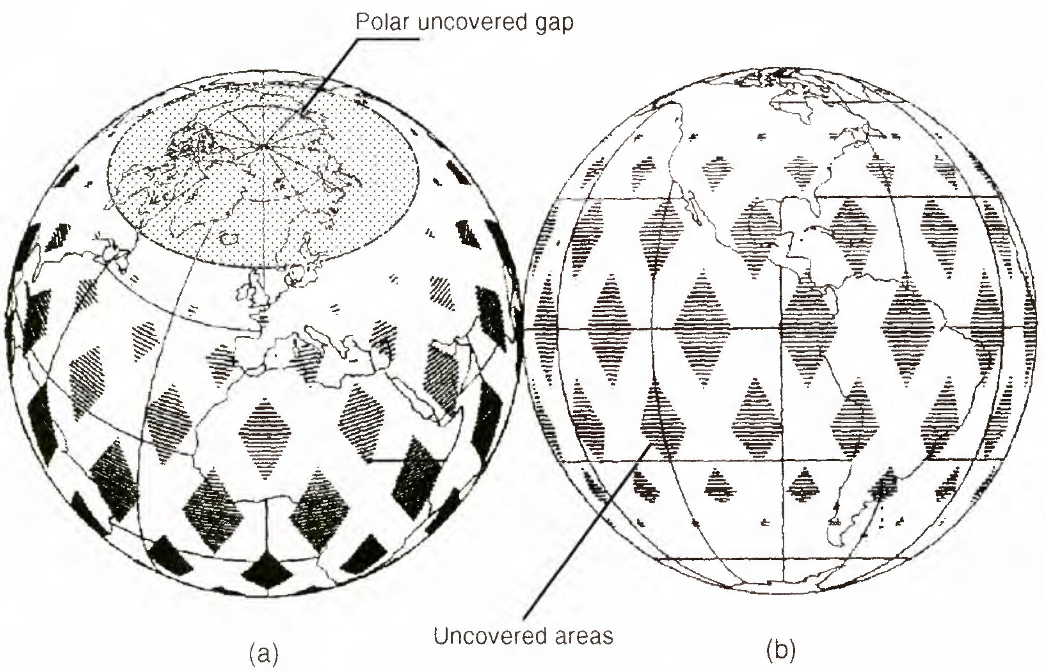

Figure 6.6: *Coverage over Europe (a) and over the Equator (b) (radiometer with 1000 km swath)*

The chosen orbit will repeat exactly the same orbit track over the Earth during the whole mission. This will leave some areas of the Earth very well covered and some other areas never covered. A solution to this problem will be to allow a gentle decay of the orbit – by a few hundred of meters – this will produce a very slow drift of the orbital tracks so that the 21 % Earth area uncovered changes with time. The altitude can be controlled such that any area is visible from several month to several years.

6.4. The Spacecraft

A life time of 5 years is assumed but the consumables have been budgeted for 6 years. Two Pre-Phase A level study contracts were carried out in 1995. The material produced has been used to provide the information contained in this chapter.

6.4.1. Configuration and Mechanical Design

The configuration of the Precipitation Mission satellite is driven by its large antenna, its low flying altitude and its non sun-synchronous orbit. Work already performed allows a number of alternatives to be identified. A possible configuration is shown in Figure 6.8. The satellite has been configured 'slender' along the velocity direction to minimise aerodynamic drag. The solar array is on the velocity face – with rotation also around the velocity axis – the Rain Radar is on the anti-velocity face, the microwave radiometer and the imager are at the top (-X), and the interface with the launcher at the bottom (+X). The Rain Radar antenna is shadowed from the wind by the body of the spacecraft. This does not improve the drag but reduces the unbalanced aerodynamic torques that must be compensated by the attitude control system of the spacecraft (see Section 6.4.2 for details).

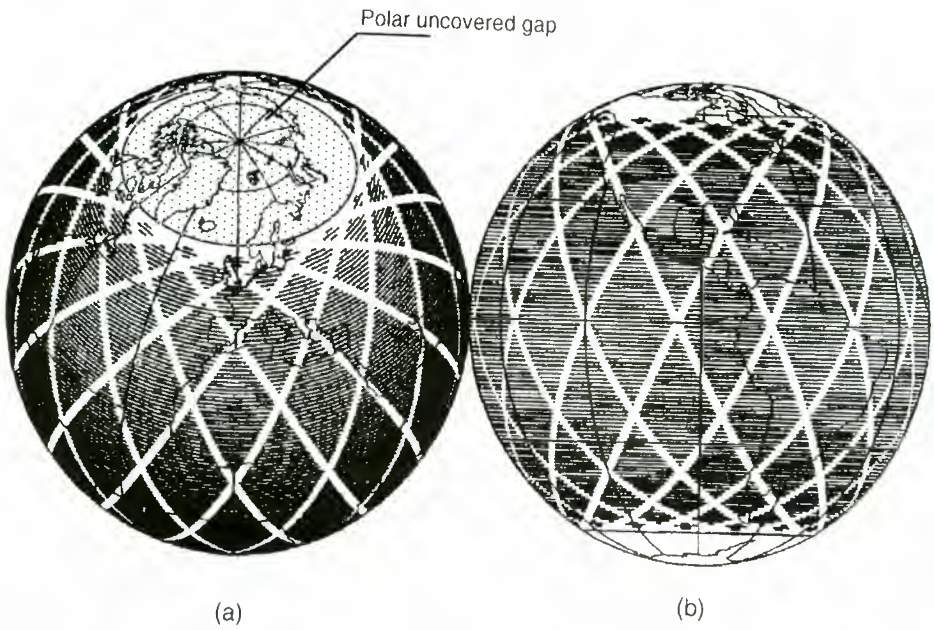

Figure 6.7: *Coverage over Europe (a) and over the Equator (b) (rain radar with 250 km swath)*

The satellite is in a non sun-synchronous orbit. To face the sun, the solar array could rotate around roll (velocity), yaw (anti-Earth) or pitch axis. If the rotation is done around roll, to be able to provide power during all seasons, a two axes gimballed solar array is needed. If the rotation is around roll or yaw, only one rotation axis is needed. Yaw axis rotation will generate very high aerodynamic imbalances; therefore motion around roll is the best alternative.

To be able to protect the antenna against the wind, the body of the spacecraft must be sized accordingly. This allows a mechanically simple Rain Radar. The feed horn line can be fixed to the spacecraft body, and the antenna needs a triple line of hinges for stowage around the spacecraft.

The expected mass budget is as follows:

Mech. and Thermal (kg)	AOCS (kg)	Power (kg)	OBDH and Telecom. (kg)	Payload (kg)	Fuel (kg)	Total (kg)
470	200	500	90	570	300	2130

Table 6.7: The Overall Mass Budget

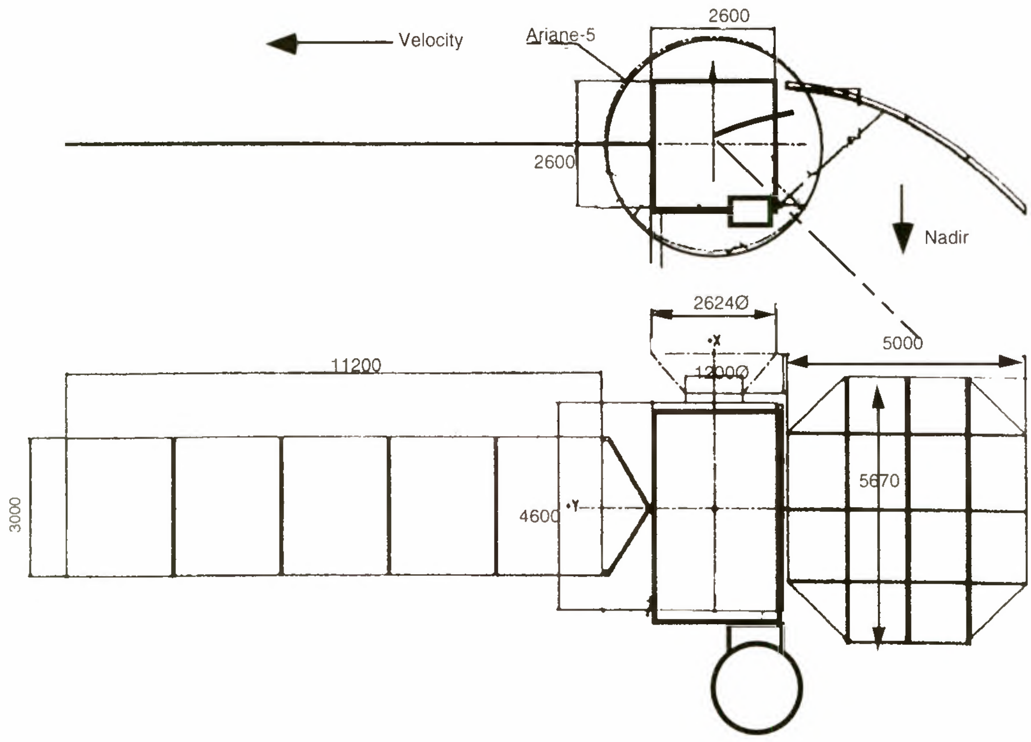

Figure 6.8: Possible Configuration of the Precipitation Explorer

In a non sun-synchronous orbit the sun can be anywhere. An evaluation of the heat rejection capabilities of the different sides of a satellite on a 60° inclination orbit has been performed and a surface of 5 m^2 of radiators on faces +Y and +Z is able to dissipate the heat. This is compatible with the space available – up to 11 m^2. All the other faces would be thermally isolated.

6.4.2. Attitude and Orbit Control

At an altitude of 500 km the corresponding air density is 2.28×10^{-12} kg m^{-3}; for a satellite with a cross section of 15 m^2, and a drag coefficient of 2.5 the resulting drag force is 2.5 mN. With 2130 kg of satellite mass, it will need 217 kg of Hydrazine for 6 years of orbit maintenance. The configuration shown – Rain Radar in the -Y side – minimises aerodynamic torques. If the Rain Radar antenna was located in the +Y (velocity) side, the high torques generated could be incompatible with a conventional attitude control system. The aerodynamic torques and forces can be seen in Table 6.8:

	Air drag torque (10^{-3} Nm)		
Configuration	Roll (X)	Pitch (Y)	Yaw (Z)
Antenna on +Y	25	1	1
Antenna on -Y	8	0.8	1.4
		Momentum (Nms)	
Antenna on -Y	4.6	2.2	2.2

Table 6.8: *The Aerodynamic Torques and Forces*

The mission derived requirements for the pointing of the satellite are not specially demanding. they can be seen here below:

Absolute pointing error (95%)	50 mrad
Absolute pointing knowledge (95%)	Roll 1.8 mrad, pitch and yaw 6 mrad
Attitude stability (95%)	1.35 mrad/s
Attitude rate knowledge (95%)	1 mrad over 3 s.
Rain Radar geolocalization	4.16 km (horizontal), 0.4 km (vertical)

Table 6.9: *Satellite Pointing Requirements*

An attitude control system almost identical to Mark-II of Spot-4 can be baselined. Gyros provide attitude measurements on the three axis. These measurements are updated by an Earth sensor in roll and pitch and by a sun sensor in yaw. External torques are compensated by the reaction wheels which are in turn off-loaded by magneto-torquers. A 40 Nms wheel per axis and two 300 Am^2 magneto-torquers on roll and pitch are sufficient. Nevertheless the changing sun position, associated to the non sun-synchronous orbit will force, either mounting one sun sensor on the solar array or working with three sun sensors, two with their axis along pitch and the third along roll. The sun sensors need a wide field of view and they must be different from the Mk-II reference but there are adequate ones available. An interesting option is to add another antenna to the GPS receiver on-board. It would be located on the spacecraft anti-Earth side, and would provide a permanent yaw attitude measurement whatever the season. The accuracy would typically be around 5 mrad.

6.4.3. Data Handling and Communications

The data rates generated by this mission are moderate. The total data rate is 620 kbps for a 200 km swath. The instrument are continuously operating and produce 3.7 Gbits per orbit and 51 Gbit per day. The communication structure will be conventional 4 kbps S band for operational up- and downlinking and 100 Mbps X band for downlinking of the payload data stream. The data handling system will be centred around a solid state mass memory. The mass memory shall be dimensioned to store the data generated during the blind period without ground contact. A total on-orbit storage of 50 Gbits is foreseen.

6.4.4. Electric Power

The power subsystem is conventional but requires a large size solar array because of the chosen orbit and array configuration, the efficiency will be half of that for a sun synchronous case. The power budget of the mission is the following:

Thermal (W)	AOCS (W)	OBDH and Telecom (W)	Payload (W)	Total (W)
50	230	125	540	945

Table 6.10: *The Overall Power Budget*

The solar array size determination shall take into account the lack of efficiency associated to the non sun-synchronous orbit. Including reasonable safety factors and dissipations on the power subsystem the solar array should be able to provide 5 times the average power. Resulting maximum solar array power shall be 4900 W. This requires between 35 and 50 m^2 depending on the technology used. The configuration depicted in Figure 6.8 is for a satellite with 36 m^2 of higher efficiency GaAs cells. The satellite should include 75 kg of batteries in NiCd with a depth of discharge of 30% working at 28 V and with a capacity of 120 Ah.

6.5. Ground Segment and Data Processing

The ground segment described corresponds to the scientific requirements but not including quick delivery of data products. This simplifies the ground segment and the data processing but limits the mission applications. To increase the usefulness of the mission direct broadcast of the measured data during overpass can be implemented as an option. This is described in Sub-section 6.5.4.

For the mission profile defined for this mission, a mid latitude European ground station, e.g.: Darmstadt is optimally located. It will provide 60 min per day of contact, 45 % of the orbits are visible and there would be an average contact time of 9 min per overpass. The mission control and management could be carried out by ESOC. The architecture of the ground segment can be seen in Figure 6.9.

6.5.1. Control and Operations

The satellite will have a high degree of autonomy; routine maintenance will be done with on-board systems. The command duty cycle is assumed to be larger than 72 hours for routine operations.

6.5.2. Data Products

The level of data to be produced are the following:

- Level 0 - raw payload data as telemetered from the satellite.
- Level 1a - 'de-packetised' data, sorted in files with calibration data attached but no correction performed.
- Level 1b - calibrated and corrected. They will be calibrate backscattering profiles for the Rain Radar and apparent temperatures for PMR.
- Level 2 - geophysical products, namely
    1) twice a day snapshots of the precipitation fields;
    2) monthly averages of the precipitation fields covering the full globe with a resolution of 250 by 250 km^2.

Data archiving would be done at level 1a. It can be assumed that the data volume will be in the same range as the raw data. This will produce a volume of 366 Tbits per year of level 1a data. Archived data would be available for delivery on request for the duration of the mission.

6.5.3. Status of Synergetic Algorithms

Swath broadening is fundamental to a successful Precipitation Mission since only with the radiometer can the precipitation be observed in a significant part of the world (more than 78%). This technique makes use of the rain radar to improve the accuracy of the radiometric retrieval (see Section 4.4) being developed within the frame of TRMM. They will soon become available. For the proposed Precipitation Mission significant improvements on TRMM will be achievable because the precipitation retrieval from the dual-frequency radar will allow the correction of PIA and the identification in the vertical precipitation profiles of particle types (e.g. water or ice). This will lead to better swath broadening algorithms. Preliminary work on this technique has already started however effort will have to put on implementing it.

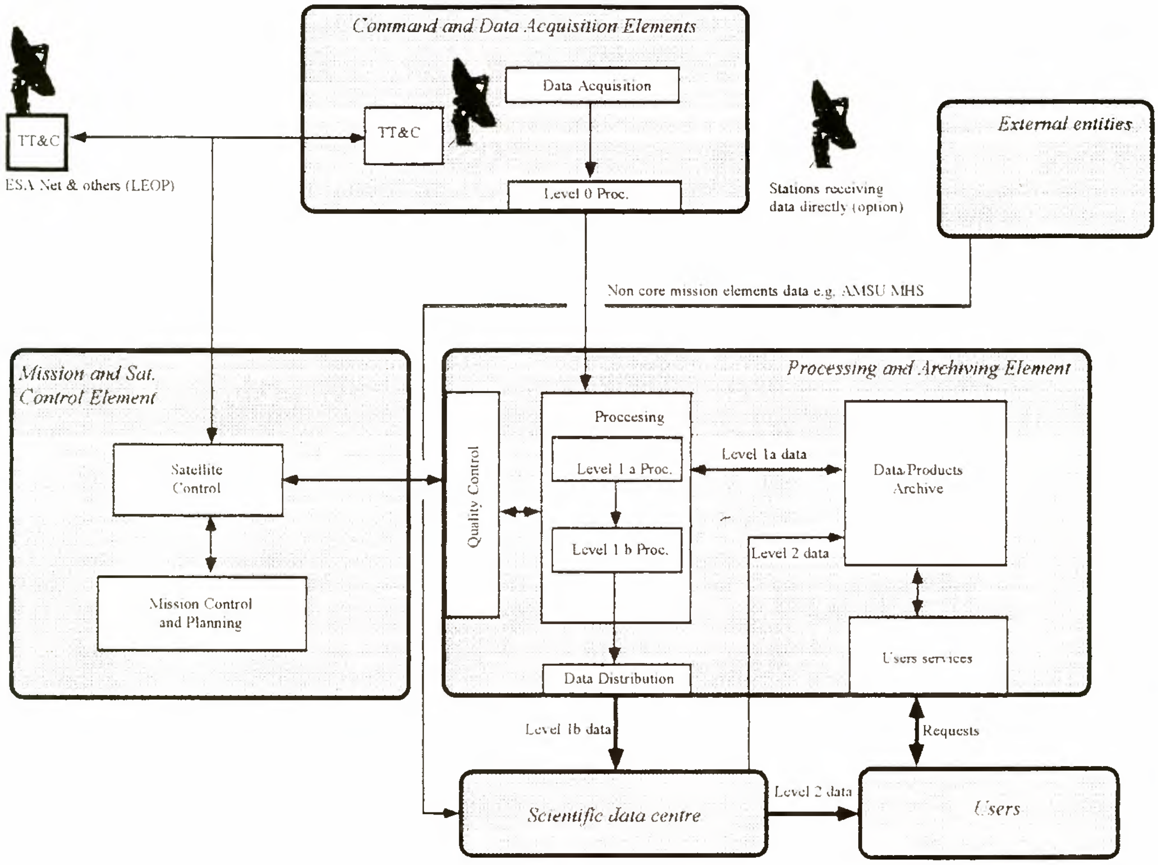

Figure 6.9: *Ground Segment Architecture*

6.5.4. Direct Data Delivery Option

The raw data produced by the Radar and the PMR could be directly broadcasted as they are produced. This would allow users to receive data on their own rain situation as the satellite flies directly over them. HRPT (high resolution picture transmission) and LRPT (low resolution picture transmission) are widely used meteorological communication standards which could be used to perform this function. Present HRPT can downlink up to 3.5 Mbps and LRPT up to 72 kbps. This should be studied as an option during Phase A.

6.6. Launcher

The satellite and rain radar described above are compatible only with a launch in Ariane-5. The large volume provided by the launcher has been used to simplify the mechanical design of the Rain Radar. Ariane-5 is able to put more than 10,000 kg in the orbit requested by the Earth Explorer Precipitation Mission. One possibility would be to arrange a shared launch. However, the sharing of a single launcher by two satellites would only be possible if both are injected in orbits with relatively similar orbit inclinations.

Another alternative would be to constrain the overall dimensions of the satellite to the volume allowed by a smaller and cheaper launcher whose load carrying capability should be compatible with the needs, e.g. Delta-II, HII or European equivalent.

In this case the deployment mechanisms of the Rain Radar is much more complicated but the reduction in launching costs will much more than compensate for the development of a mechanically complex Rain Radar. This should be reviewed during Phase A.

6.7. Implementation Option

An alternative implementation for the Precipitation Mission has recently been studied. In this configuration the Precipitation Radar (PROMES - Precipitation Radar - conical mechanical scanning) uses a mechanical scanning antenna with a 4.5 m diameter and a boresight angle of 14° off nadir that ensures a swath of 250 km for a satellite height of 500 km. A characteristic of this solution is that the beams at 14 and 24 GHz would overlap perfectly. Precipitation retrieval is simplified because the incidence angle is constant. The layer from the ground that would not be observable (blind layer) due to the antenna beamwidth and its non-zero incidence angle would be about 1.2 km.

The antenna is a prime-feed offset reflector antenna. For the reflector antenna to have good scanning capabilities a f/D ratio of 0.8 is used. Since the beam should perform a conical scan, an offset geometry has been selected where the offset angle makes an angle of 14° with the axis of revolution of the generating paraboloid. Using the antenna in a tilted configuration, and spinning it around the offset axis, the main beam makes a conical scan with half opening angle of 14°. The surface area of the reflector is approximately 17 m^2 and its footprint on the surface of the Earth is 3.2 km. Using 6 dual frequency feed horns to acquire 6 adjacent scans, PROMES rotates approximately at 23 rpm to achieve full coverage of the 250 km swath. This rotation speed is consistent with the mechanisms developed for PMR and its technological risk is minimal. The RF part, feeds and antenna will all be in rotation. The side lobe levels for each of the beams satisfies the requirement of better than 30 dB below the main lobe in those areas where it cannot be eliminated by time-domain processing.

In principle, the radar would be in operation only during half of the conical scan with all six feeds. However, stereoscopic observation of precipitation is also possible with 3 feeds. Adaptive scanning strategies with the conical scanning configuration are also relatively simple to implement and attractive since they lead to significant power savings. A possibility that would lead to a 40 % power saving would be to use only 3 feeds in the frontal part of the scan to identify the presence of rain and if rain is identified use the full 6 feeds in the back scan. This strategy would give both full and stereoscopic coverage. The estimated mass for PROMES is 265 kg while its power consumption is 355 W for full coverage with no adaptive scanning (both these estimates include also a balancing momentum wheel).

Since the boresight off-nadir angle of the PMR is much larger than the one required for the radar, it is possible to mount PMR on the zenith-side of the spacecraft while PROMES is mounted on the nadir side (see Figure 6.10). PROMES and PMR would then rotate in opposite directions to partially compensate each others angular momentum. In this configuration, GRAS is mounted on the front side of the spacecraft while the X-band antenna is mounted on the side and is deployed after launch to assume a position flush to the antenna of PROMES. The TT/C S-band antenna is mounted on the nadir side of the feed cluster of PROMES.

An advantage of this configuration is that an additional 215 km of swath width (swath width of 1236 km with a ±90° scan) can be achieved. PMR has the same antenna size as MIMR but a nadir angle of 49°. With this antenna the incidence angle on the ground is 55° and improved resolutions can be achieved due the lower height of the satellite orbit. PMR does not require a balancing wheel because its angular momentum is compensated by PROMES. The rotation speed of PMR is 32 rpm.

The solar panels, using conventional technology and having a single degree of freedom (rotation around the axis of the solar panel assembly), have an area of 46 to 50 m^2 with a width of 4 m. The lower solar panel area is necessary to satisfy the power requirements of the spacecraft when using conventional chemical propulsion while the higher figure is for electrical (ion thruster) propulsion. AOCS of Mk-II, Spot-IV, type is adequate.

The launch configuration uses a single satellite Ariane-5 launch. The satellite within the Ariane-5 faring is shown in Figure 6.11.

The power requirements for this configuration are similar to those in the baseline of Section 6.4, however the total launch mass is 1475 kg. The savings in mass are achieved by using a much smaller platform. This is possible due to the different configuration and lower mass and size of the precipitation radar. Detailed budgets can be seen below:

Mech. and Thermal (kg)	OBDH and Telecom (kg)	Power (kg)	AOCS and Propulsion (kg)	Payload (kg)	Fuel (kg)	Total (kg)
275	90	335	190	435	150	1475

Table 6.11: *Tentative Mass Budget for PROMES*

Thermal (W)	OBDH and Telecom (W)	AOCS and Propulsion (W)	Payload (W)	Total (W)
50	125	300	560	1035

Table 6.12: *Tentative Power Budget for PROMES*

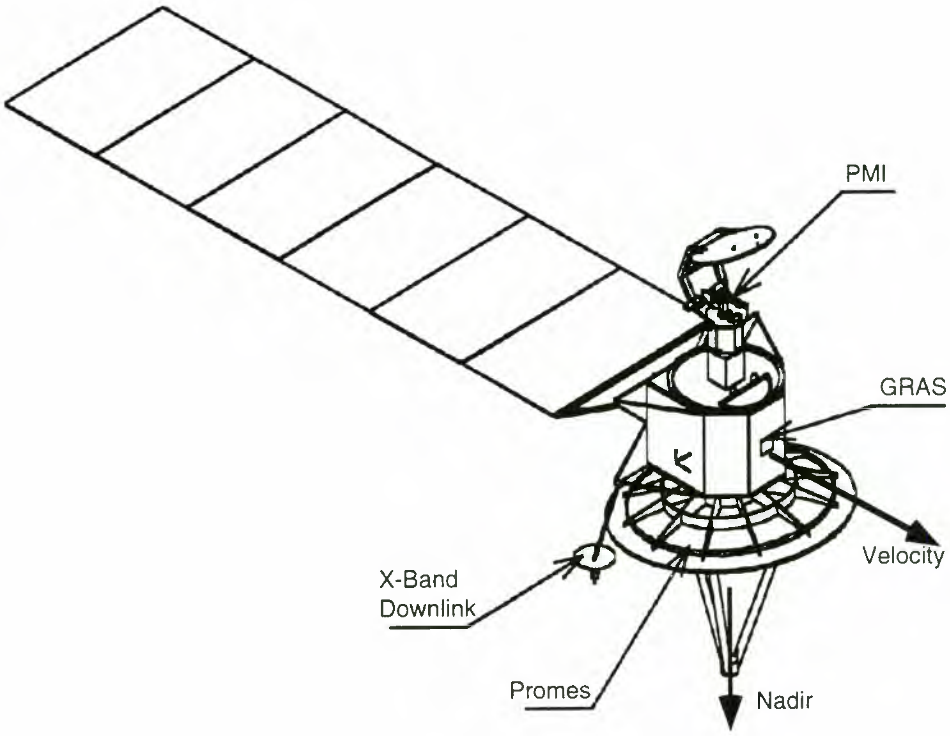

Figure 6.10: Tentative Configuration for the PROMES Concept

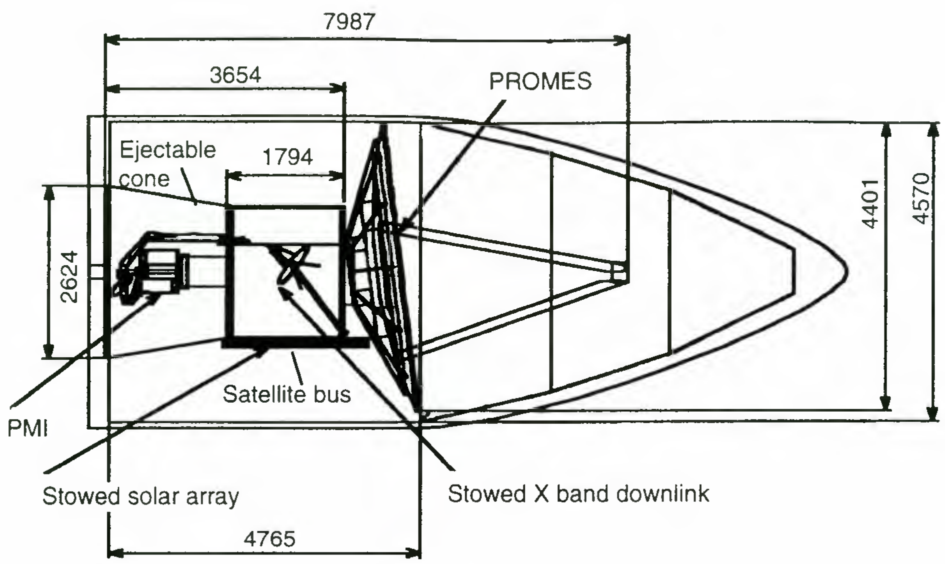

Figure 6.11 Satellite Dimensions

7. Programmatics

7.1. General

The Precipitation Mission would be implemented in the frame of an ESA Earth Explorer Programme of research missions if selected after phase A studies carried out within the framework of the Agency's Earth Observation Preparatory Programme.

7.2. Critical Areas and Open Issues

The development of the electronically scanning Rain Radar has reached the level of instrument concept definition. The option with mechanical scanning is less developed. In both cases, it is a complex instrument with challenging electric and mechanical problems. The electronically scanning option will require the development of a complex dual frequency electronic scanning and of a large size deployable antenna.

These problems are alleviated in the mechanically scanning alternative as electronic scanning is not needed but the antenna is still big and has to rotate. The experience acquired with the MIMR demonstrator and with developments on contactless transmission systems is applicable.

The PMR will be built on the MIMR concept. There is a strong technology development underlying this and no new challenges are anticipated.

The satellite itself is challenging as it is a large spacecraft flying at a relatively low altitude and mid inclination with the associated issues of drag effects, varying illumination conditions and their implications on thermal and power systems. The accommodation of the large deployable antenna is the main configuration driver if the electronic scanning radar is used. For the option with the mechanically scanning radar the accommodation of the antenna is less difficult but the control of the satellite with two large rotating masses has to be further investigated.

In summary, this would be a medium to large mission requiring developments at platform and instrument level.

7.3. Related Missions and Timeliness

The US/Japan cooperation TRMM (1997) and the ATMOS-A1(2003) of Japan are missions of similar and/or complementing nature. Objectives and observation capabilities are similar to those for the Precipitation Mission which, with its dual frequency scanning radar, would enhance the capability to operate over land as well as ocean. The higher inclination of the

Explorer would also allow study of precipitation systems over Europe and generally mid-latitude regions of the world.

TRMM is in phase C/D and will be launched in 1997. The results from TRMM would help the definition of the Precipitation Mission.

Also related to the Precipitation Mission are the geostationary and polar meteorological missions by providing auxiliary data required to fulfil the scientific objectives.

The time for the launch of the Precipitation Mission should take into account the development effort for a mission of this class and the time required to exploit the results of TRMM. A launch in 2003/2004 should meet these criteria and would also allow it to operate around the minimum solar activity (2006) of the next solar cycle, which would be beneficial taking into account the low orbit altitude.

7.4. International Cooperation

As indicated above studies and monitoring of precipitation attract international interests. Beyond TRMM, there would be the ATMOS-A1 mission – still at a conceptual level – and the Earth Explorer Precipitation Mission. Given the possible complementarities and/or similarities of these missions, there would be scope for international cooperation spanning from a dual satellite mission to increase spatial and temporal coverage to other forms of cooperation for a single satellite with contributions from partners - this would be studied during Phase A.

7.5. Enhancement of European Capabilities and Applications Potential

The Precipitation Mission will aid interpreting data from polar and geostationary imagers and sounders thus enhancing their operational value. The mission will develop passive and active microwave techniques for precipitation observation. This capability was identified by the EU Panel of Experts on Satellites of the WMO already in 1991 as a long term requirement for operational meteorology in the frame of a statement of general requirements for the space-based subsystems of the Global Observing System.

The developments required for the Earth Explorer Precipitation Mission will provide valuable technology in the areas of active and passive microwave instrumentations and platforms. In particular, it would provide a flight opportunity for an instrument derived from the developments and investments made for MIMR and establish both from the user and industrial point of view a basis for longer term continuous monitoring of precipitation.

References

Amayenc, P., J.-P. Diguet, M. Marzoug, and T. Tani (1996): A class of single and dual-frequency algorithms for rain rate profiling from a spaceborne radar. Part II: Tests for airborne radar measurements, *J. Atmos. Ocean. Technol.*, **13**, 142-164 (in press)

Arkin, P.A., R. Joyce and J.E. Janowiak (1994): The estimation of global monthly mean rainfall using infrared satellite data: The GOES Precipitation Index (GPI), *Remote Sens. Rev.*, **11**, 107-124.

Atlas, D., D. Rosenfeld, A.R. Jameson (1995): Evolution of Radar Rainfall Measurements: Steps and Mis-steps, *III Int. Conf. on Hydrological Applications of Weather Radar,* Sao Paulo, Brazil, August 20-24, 1995

Capsoni, C., F. Fedi, and M. Paraboni (1987): Data and theory for a new model of the horizontal structure of raincells for precipitation applications, *Radio Sci.*, **22**, 395-404

Cheng, M. and R. Brown (1995): Delineation of precipitation areas by correlation of Meteosat visible and infrared data with radar data, *Month. Weather Rev.*, **123**, 2743-2757

Chong, M. and D. Hauser, (1990): A Tropical Squall Line Observed During the COPT 81 Experiment in West Africa. Part III: Heat and Moisture Budget. *Month. Weather Rev.*, **118**, 1696-1706

Doneaud, A.A., P.L. Smith, A.S. Dennis, and S. Gupta (1981): A simple method for estimating convective rain volume over an area, *Water Resour. Res.*, **17**, 1676-1682

Ebert, E.E., M.J. Manton, P.A. Arkin, R.E. Allam and A. Gruber (1996): Results from the GPCP Algorithm Intercomparison Programme, *Bull. Amer. Met. Soc.*, in press

ESA (1996a): The MIMR Interim Report, (in preparation)

ESA (1996b): The Atmospheric Profiling Mission, *ESA SP-1196(7)*

Goldhirsh, J. and B.H. Musiani (1986): Raincell size statistics derived from radar observations at Wallops Island (Virginia), *IEEE Trans. Geo Sci. Remote Sens.*, **24**, 947-954

Guissard, A., P. Sobieski, C. Baufays (1992): A unified approach to bistatic scattering for active and passive remote sensing of rough ocean surfaces, *Trends in Geophys. Res.* , **1**, 43-68

Hitchfeld, W. and J. Bordan (1954) : Errors inherent in the radar measurement of rainfall at attenuating wavelengths, *J. Meteorol.*, **11**, 58-67

Hollinger, J.P., J.L. Peirce and G.A. Poe (1990): SSM/I instrument evaluation, *IEEE Trans. Geosci. Remote Sensing*, **28**, 781-790

Kabèche, A., and J. Testud, (1995): Stereoradar meteorology: a new unified approach to process data from airborne or ground-based meteorological radars, *J. Atmos. Ocean. Technol.*, **12**, 783-799

Igushi, T. and R. Meneghini (1994): Intercomparison of single frequency methods for retrieving a vertical rain profile from airborne or spaceborne radar data, *J. Atmos. Ocean. Technol.*, **11**, 727-737

Lovejoy, .S and G.L. Austin (1979): The delineation of rain areas from visible and IR satellite data from GATE and mid-latitudes, *Atmos. Ocean.*, **17**, 77-92

Legates, D.R. and C.J. Willmott (1990): Mean seasonal and spatial variability in gauge-corrected global precipitation, *Int. J. Clim.*, **10**, 111-127

Marshall, J.S. and W.M.K. Palmer (1948): The distribution of raindrops with size, *J. Meteorol.*, **5**, 165-166

Marzano, F.S., A. Mugnai, E.A. Smith, X. Xiang, J. Turk and J. Vivekanandan (1994): Active and passive remote sensing of precipitating storms during CaPE. Part II: Intercomparison of precipitation retrievals over land from AMPR radiometer and CP-2 radar, *Meteorol. Atmos. Phys.*, **54**, 29-51

Marzoug, M. and P. Amayenc (1994): A class of single- and dual-frequency algorithms for rain rate profiling from a spaceborne radar, Part I: Principle and tests from numerical simulations, *J. Atmos. Ocean. Technol.*, **11**, 1480-1505

Meneghini, R. and J.A. Jones, 1993: An Approach to Estimate the Areal Rain-Rate Distribution from Spaceborne Radar by the Use of Multiple Thresholds, *J. Appl. Meteor.*, **32**, 386-398

Meneghini, R., T. Kozu, H. Kumagai, and W.C. Boncyck (1992): A study of rain estimation methods from space using dual-wavelength radar measurements at nadir incidence over ocean, *J. Atmos. Ocean. Technol.*, **9**, 364-382

Meneghini, R. and K. Nakamura (1990): Range profiling of the rain rate by an airborne weather radar, *Remote Sens. Environ.*, **31**, 193-209

Prigent, C., A. Sand, C. Klapisz , Y. Lemaitre (1994): Physical Retrieval of liquid water contents in a North Atlantic Cyclone Using SSM/I data, *Q. J. Meteoröl. Soc.*, **120**, 1179-1207

Simpson, J., R.F. Adler and G.R. North (1988): A proposed Tropical Rainfall Measuring Mission (TRMM) satellite, *Bull. Amer. Met. Soc.*, **69**, 278-295

Smith, E.A., J. Chang and J. Lamm (1995): PIP-2 Intercomparison Results. Report, Dept. of Meteorology, Florida State University, Tallahassee, Florida, USA

Smith, E.A., C. Kummerow and A. Mugnai, 1994: The emergence of inversion-type profile algorithms for estimation of precipitation from satellite passive microwave measurements. *Remote Sens. Rev.*, **11**, 211-242

Spencer, R.W., R.E. Hood, F.J. La Fontaine, E.A. Smith, R. Platt, J. Galliano, V.L. Griffin and E. Lobl (1994): High-resolution imaging of rain systems with the Advanced Microwave Precipitation Radiometer, *J. Atmos. Oceanic Technol.*, **11**, 849-857

Tani, T. and P. Amayenc (1995): Tests of algorithms for range profiling of the rain rate from ARMAR data in TOGA-COARE, *27th Radar Meteorology Conference*, Oct. 9-13, Vail (Co), 789-791

Testud, J., P. Amayenc, X.-K. Dou, T. Tani (1996): Tests of rain profiling algorithms from a spaceborne radar using raincell models and real data precipitation fields, *J. Atmos. Ocean. Technol.*, **13**, 426-453, in press

Webster, P.J., and R. Lucas (1992): TOGA COARE: The Coupled Ocean-Atmosphere Response Experiment, *Bull. Amer. Met. Soc.*, **73**, 1377-1416

Wilheit, T., R. Adler, S. Avery, E.C. Barrett, P. Bauer, W. Berg, A. Chang, J. Ferriday, N. Grody, S. Goodman, C. Kidd, D. Kniveton, C. Kummerow, A. Mugnai, W. Olson, G. Petty, A. Shibata, E.A. Smith and R.W. Spencer (1994): Algorithms for the retrieval of rainfall from passive microwave measurements, *Remote Sens. Rev.*, **11**, 163-194

List of Acronyms

ACSYS	Arctic Climate System Study
AIP	Algorithm Intercomparison Project
AMPR	Advanced Microwave Precipitation Radiometer
AMSU	Advanced Microwave Sounding Unit
AMSR	Advanced Microwave Scanning Radiometer
AOCS	Attitude and Orbit Control System
ARMAR	Airborne Rain Mapping Radar
CAPE	Convection and Precipitation/Electrification Experiment
CERES	Clouds and the Earth's Radiant Energy System
COARE	Coupled Ocean-Atmosphere Response Experiment
DMSP	Defence Meteorological Satellite Program
ECMWF	European Centre for Medium Range Weather Forecasts
ERA	ECMWF Re-analysis
ERBE	Earth Radiation Budget Experiment
EWC	Equivalent Water Content
GARP	Global Atmosphere Research Programme
GATE	GARP Atlantic Tropical Experiment
GCM	General Circulation Model
GNSS	Global Navigation Satellite System
GOES	Geostationary Operational Environment Satellite
GPCC	Global Precipitation Climate Centre
GPCP	Global Precipitation Climatology Project
GPI	GOES Precipitation Index
GRAS	GNSS Receiver for Atmospheric Sounding
HIRS	High-resolution Infrared Sounder
HRPT	High Resolution Picture Transmission
IASI	Infrared Atmospheric Sounding Interferometer
IR	Infrared
ICLWC	Integrated Cloud Water Content
ITCZ	Innertropical Convergence Zone
IWVC	Integrated WV Content
LEO	Low Earth Orbit
LIS	Lightning Imaging Sensor
LRPT	Low Resolution Picture Transmission

MCC	Mesoscale Convective Complex
METOP	Meteorological Operational
MHS	Microwave Humidity Sounder
MIMR	Multifrequency Imaging Microwave Radiometer
MSU	Microwave Sounding Unit
MW	Microwave
NMC	National Meteorological Center
NWP	Numerical Weather Prediction
OBDH	On-board Data Handling
PDF	Probability Distribution Function
PIA	Path Integrated Attenuation
PIP	Precipitation Intercomparison Project
PMR	Precipitation Microwave Radiometer
PR	Precipitation Radar
PROMES	Precipitation Radar Conical Mechanical Scanning
SSM/I	Special Sensor Microwave Imager
SST	Sea Surface Temperature
SWS	Surface Wind Speed
TOA	Top of the Atmosphere
TOGA	Tropical Ocean Global Atmosphere
TMI	TRMM Microwave Imager
TRMM	Tropical Rainfall Measuring Mission
TT/C	Telemetry and Telecommand
VIRS	VIS IR Scanner
VIS	Visible
WCRP	World Climate Research Programme
WGNE	Working Group on Numerical Experimentation
WMO	World Meteorological Organisation
WV	Water Vapour

European Space Agency
Agence spatiale européenne

Contact: ESA Publications Division
c/o ESTEC, PO Box 299, 2200 AG Noordwijk, The Netherlands
Tel (31) 71 565 3400 - Fax (31) 71 565 5433